



**Università
degli Studi
di Ferrara**

**DOTTORATO DI RICERCA IN
SCIENZE CHIMICHE**

CICLO XXXIV

COORDINATORE Prof. Alberto Cavazzini

**Overcoming light and mass transfer phenomena in gas-
liquid biphasic reactions: introduction of the aerosol
methodological paradigm**

Settore Scientifico Disciplinare: CHIM/06

Dottoranda/o

Dott. Urbani Daniele

(firma)

Tutore

Prof,ssa Bortolini Olga

(firma)

Anni 2019/2022

Summary

Droplets morphology and properties	1
How aerosol can be produced.....	3
Medical nebulizer.....	3
Water bath ultrasound aerosol generators.....	4
Burgener nebulizer.....	5
Laskin nebulizer.....	6
Ultrasonic nozzles nebulizer.....	7
Leidenfrost droplet generator.....	8
Electrospray ionization aerosol generator.....	9
Mass monitoring and kinetics acceleration.....	10
Aerosol reaction scaled up.....	12
Aim of the PhD	17
Design and manufacture of novel reactors	20
Photochemical reactors.....	20
Carbon dioxide utilization reactors.....	24
Modular reactor for aerosol synthesis.....	28
Photochemical reactions in bulk condition	32
Singlet oxygen and previous studies.....	32
Bulk photochemical oxidation of organic sulfides with water.....	34
Solubility studies.....	34
Result and discussion.....	37
Methods.....	41
Photochemical reactions in aerosol condition	45
Carbon capture and utilization in bulk condition	53
Carbon capture and utilization in aerosol condition	60
Conclusion	70
Appendix	71

Droplets morphology and properties

The use of microflow reactors in organic chemistry has been an extremely flourishing field of research in recent years, due to the ability to enable significant improvements in the apparent rates of chemical reactions¹. The idea and the advantage that stands behind flow chemistry is to reduce the volume of the reaction solutions, compared to batch conditions, and consequently increase the reactive surface area of the liquid bulk. This is particular true in two cases:

1. photochemical reactions

where light can be absorbed within the reaction solution in a limited fraction of the reactor volume, as a consequence of the Lambert-Beer equation ($A = \epsilon cl$, where A is the absorbance, ϵ is the molar absorption coefficient^a, c is the concentration of the absorbent species and l is the optical path length);

2. biphasic gas-liquid reactions in which the gas can be bubbled into the liquid phase, with smaller bubbles enhancing the contact surface area^{2,3}.

By the way, microflow reactors have also some disadvantages like small throughputs and expensive devices to fine controlling the instrumental setup like pressure regulators, pumps, mass flow controller, etc.

This thesis will introduce aerosol reactions as an additional methodological approach to increase the reactive surface area of the reaction media.

By definition, aerosol is a fluid system of two or more components in which the dispersed phase is a solid, a liquid or a mixture of both and the continuous phase is a gas (usually air)^b. In this thesis will be discussed only aerosols in which the dispersed phase is liquid. The liquid phase in the aerosol is dispersed in microdroplets with specific properties. In studying aerosol reactions

^a IUPAC. *Compendium of Chemical Terminology, 2nd ed. (the "Gold Book")*. Compiled by A. D. McNaught and A. Wilkinson. Blackwell Scientific Publications, Oxford (1997). Online version (2019-) created by S. J. Chalk. ISBN 0-9678550-9-8. <https://doi.org/10.1351/goldbook>

^b IUPAC. *Compendium of Chemical Terminology, 2nd ed. (the "Gold Book")*. Compiled by A. D. McNaught and A. Wilkinson. Blackwell Scientific Publications, Oxford (1997). Online version (2019-) created by S. J. Chalk. ISBN 0-9678550-9-8. <https://doi.org/10.1351/goldbook>

each single droplet that forms the aerosol has to be considered as a single reactor, and droplets features are key to understand how exactly reactions take place therein.

Various nebulization techniques are currently used to disperse the liquid phase in microdroplets, each affecting droplets key features, such as:

1. the average size distribution;
2. the droplets morphology;
3. the droplets lifetime.

The most important feature of aerosol droplets is the size distribution, because the droplets size affects the droplet surface to volume ratio, that is really important when facing with reaction that are limited by mass transfer phenomena.

In biphasic gas-liquid reactions, in which the gas dissolve into the liquid through the gas-liquid interphase, the liquid surface to volume ratio is a key parameter affecting the reaction efficiency. It can be telescoped passing from classic batch reactors to continuous microflow reactors and to aerosol reactors.

In a classic batch reactor, the gas-liquid interface through which the gas dissolve into the bulk solution is only represented by the bulk liquid surface, resulting in low liquid surface to volume ratios. Stirring the reaction mixture or bubbling the gas into the liquid phase increases the extent of the gas-liquid interface, and this is the fastest method to increase the quantity of gas that can dissolve inside the solution per time units.

Compared to classic batch reactors, in microflow reactors the gas-liquid interface increases when operating in plug-flow mode in which alternate gas and liquid segments are axially injected into the tubular reactor.

In aerosol the roles of liquid and gas phases are actually reversed: a small amount of liquid is completely surrounded by the gas causing a significative increase of the gas-liquid interface that result in a surface to volume ratio increase by several order of magnitude.

The study of aerosol droplet morphology is difficult task, and can be done only using expensive high resolution cameras or laser diffraction methods. At the best of our knowledge, there are no evidences in the literature questioning the spherical shape of mechanically nebulized solution,

and for the rest of this thesis, we can safely assume that this is the only shape that droplet will have in the aerosol.

Another parameter that is really important is the droplets lifetime, namely the average time that last each droplet, from the nebulization to the back-condensation into a liquid phase. It only depends on the reactor design, size and, eventually, the gas flow. It is not possible to follow one or more droplets from the moment they are generated until the back-condensation occurs but, at the best of our knowledge, this time can also be approximated. The average droplets lifetime can be estimated by measuring the time that goes from the starting of the nebulization process until the droplets reach the condensation facilities of the reactor.

Microdroplets can be easily observed with a simple light torch through diffraction phenomena.

How aerosol can be produced

There are several methods to nebulize a liquid solution, but all of those just belong to two categories: mechanically induced aerosol or electrospray mechanism.

Medical nebulizer

Medical nebulizers are the easiest and cheapest devices that can be used to nebulize a solution. These devices are commonly sold in pharmacies and used to treat various diseases through the aerial administration of drugs. Medical nebulizers work through Venturi effect: the carrier gas, flowing through a small tube, produces a reduced pressure over a second small tube, one end of which is immersed in the nebulizing liquid; this pressure gap allows the suction of the liquid that is then converted into an aerosol by the carrier gas. Several type of medical nebulizers can be easily found on the market, with or without a droplet size cut-off system, that is used to back-condense oversized generated droplets. These devices usually produce droplets of 10-15 μm . One big disadvantage of medical nebulizer is their durability and the fact that they can only be used in continuous flow conditions. Two typical medical nebulizers are depicted in Figure 1.

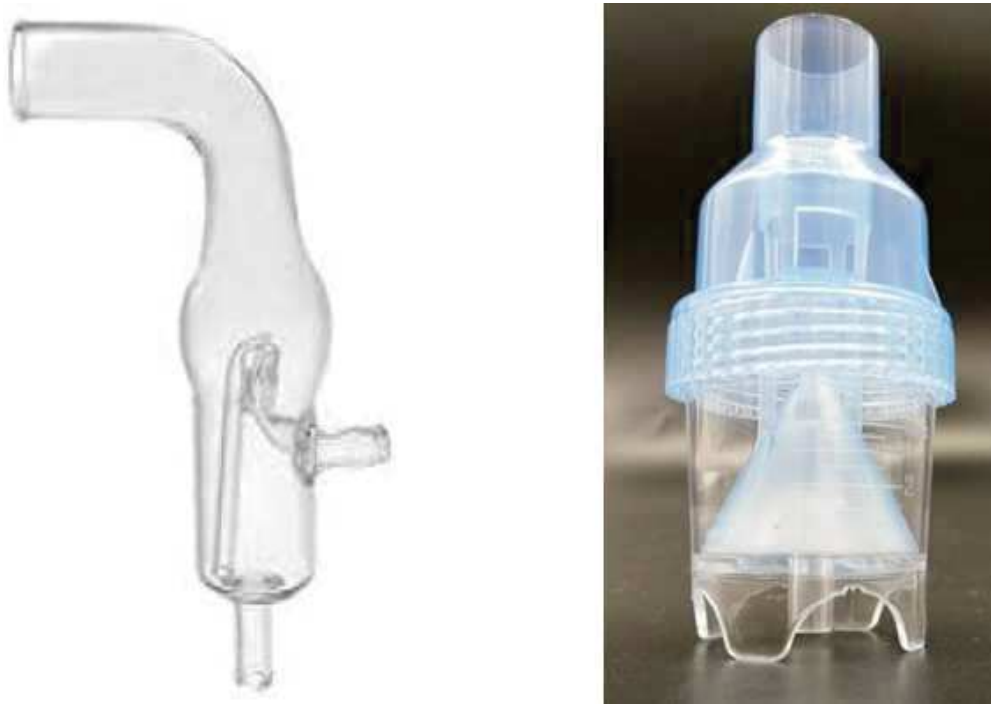


Figure 1: *Typical medical nebulizers available on the market.*

Water bath ultrasound aerosol generators

Several type of ultrasound aerosol generators can be found on the market, with different operating mechanism, the most common of which uses a piezoelectric transducer immersed in a water bath to generate the aerosol. A piezoelectric transducer, driven by electric current, start vibrating at a pre-set frequency, which determine the droplets average size: higher frequencies generate smaller droplets. The water bath transmits vibrations to a thin plastic film, that is transparent to the ultrasound and is flexible. The liquid nebulizing solution is placed on the opposite side of the film, and is nebulized accordingly to the frequency used and the viscosity of the solution: high viscous liquids need really high frequencies to be nebulized. With this device it is possible to regulate some parameters affecting microdroplets properties:

1. the current intensity flowing into the piezoelectric transducer, affecting the transducer vibration frequency;
2. the flow of the carrier gas, that can be added directly from the machine.

Usually these devices are plastic made, severely limiting the range of suitable organic solvent and reagents. Pre-fitting adaptations are needed in those cases, for instance the plastic film replacement with thin aluminum foils compatible with chemicals and solvents. A commercially available device is reported in Figure 2.



Figure 2: *Commercially available ultrasound aerosol generators.*

Burgener nebulizer

The Burgener nebulizer is one of the most advanced type of mechanical nebulizer on the market. Most of the Burgener nebulizers are in Teflon to resist to chemicals and corrosive solutions. The carrier gas and the liquid phase are pumped into two coaxial channels inside the core of the nebulizer and they meet each other at the head of the nebulizer. In this case the aerosol is formed by the combined effect of the small orifice where the liquid exit the nebulizer and the gas flow that is directed at a precise angle to impact the liquid flow. This type of nebulizer is quite expensive and cannot be use on his own but needs to be coupled, at least, with an high precision pump and a mass flow controller. This devices are all necessary because aerosol formation is assured only with precise combination of gas and liquid flows. In Figure 3 a Burgener nebulizer specification are reported.

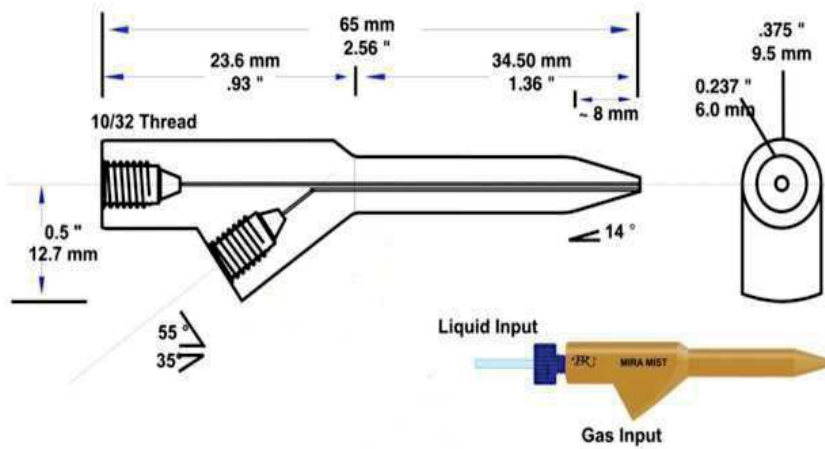


Figure 3: Commercially available Burgener nebulizer.

Laskin nebulizer

The Laskin nebulizer is another type of nebulizer that exploits the Venturi effect. Although the theoretical base behind this device is similar to that of medical nebulizer, the way it works is quite different and deserve a dedicated description. This particular nebulizer consists of a steel tube that has four holes (diameter 1 mm) arranged symmetrically and radially, perpendicular to the axis of the nozzle tube. Near the holes from which the pressurized gas comes out, there is a disc with a larger diameter in which 4 holes (2 mm diameter) have been drilled along the axis of the nozzle itself. The nozzle inserted into the container is completely immersed in the solution that needs to be sprayed. In a similar way to the medical nebulizer, also in this case the carrier gas reduces the pressure near the hole facilitating, in this way, the suction of the liquid. A commercially available Laskin nebulizer is reported in Figure 4.



Figure 4: *Commercially available Laskin nebulizer.*

Ultrasonic nozzles nebulizer

This kind of nebulizers exploits the same theory of the water bath ultrasound aerosol generator, but in this case there is no piezoelectric transducer and water bath. Basically, the instrument has a needle or a thin tube that vibrates at high frequencies generating the aerosol when liquid is pumped through. Vibration frequency and droplet size are inversely correlated: the higher the frequencies, the smaller the droplets. Of course an high precision pump is needed to guarantee a steady and reproducible aerosol. A commercially available ultrasonic nozzle nebulizer is reported in Figure 5.



Figure 5: *Commercially available ultrasonic nozzle nebulizer.*

Leidenfrost droplet generator

This droplet generator actually does not work as a nebulizer, but it is important in this discussion because the Leidenfrost effect was widely studied in the scientific literature for a better understanding of droplet reactivity⁴⁻⁶. The Leidenfrost effect is a physical phenomenon in which a liquid, placed over a surface with a temperature higher than the liquid boiling point, produces an insulating vapor layer that keeps the liquid from boiling rapidly. Because of this repulsive force, is virtually impossible to think about a scale up or a lab scale reactor to perform organic chemistry reactions, however the Leidenfrost droplet generator was a breakthrough in the study of small droplet behavior and reactivity in the past decades. In Figure 6 Leidenfrost effect explained graphically.

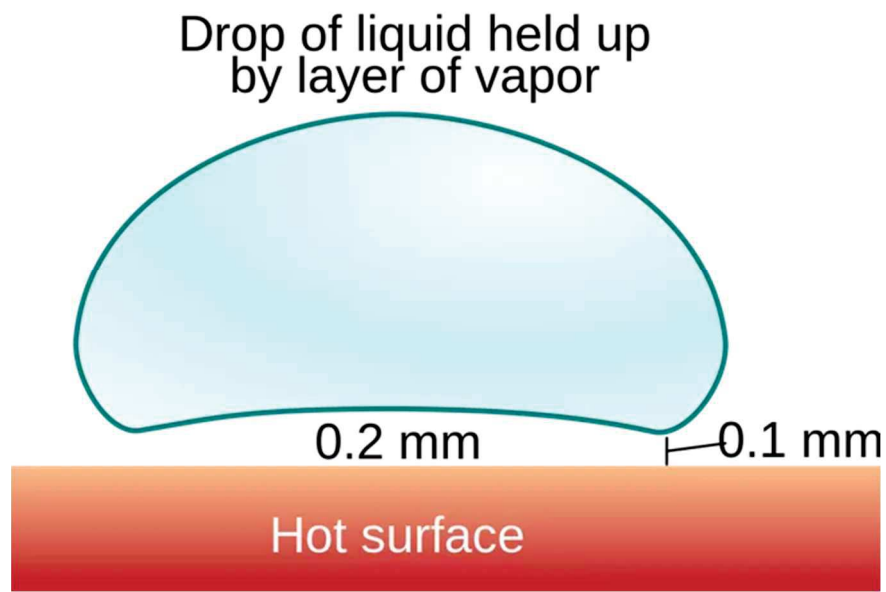


Figure 6: *Leidenfrost effect.*

Electrospray ionization aerosol generator

In electrospray ionization (EI) the aerosol is generated in completely different way from the methods described above. In this case the aerosol is formed by applying an high voltage to a liquid that, when charged, will explode due to coulombic repulsion into charged droplets. This kind of generator is extensively used in mass spectroscopy techniques in the field of analytical chemistry. This approach is particularly interesting for organic chemistry because it gives the possibility to easily study the reactions mechanism. Thus, with this approach it is possible to identify reaction intermediates and catalyts behavior. An important point that needs to be taken in consideration is that the droplets generated are charged and so the environment where the reaction takes place is completely different from a classical batch reactor. Having said that a direct comparison between different setups can be difficult and can led to misinterpretation on reaction mechanism. In Figure 7 a detail of EI nebulizer is coupled with a mass spectrometer is reported.

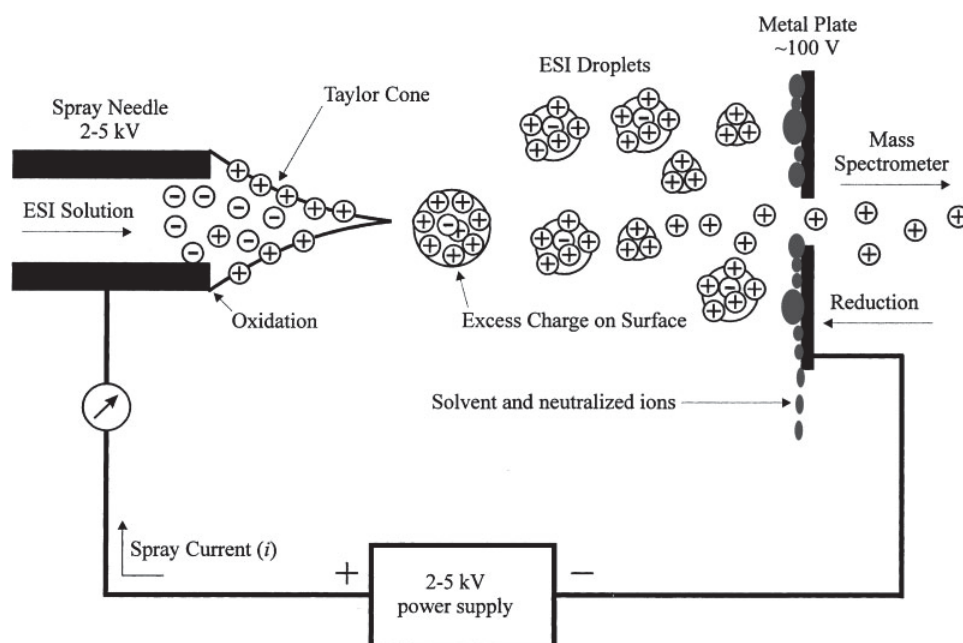
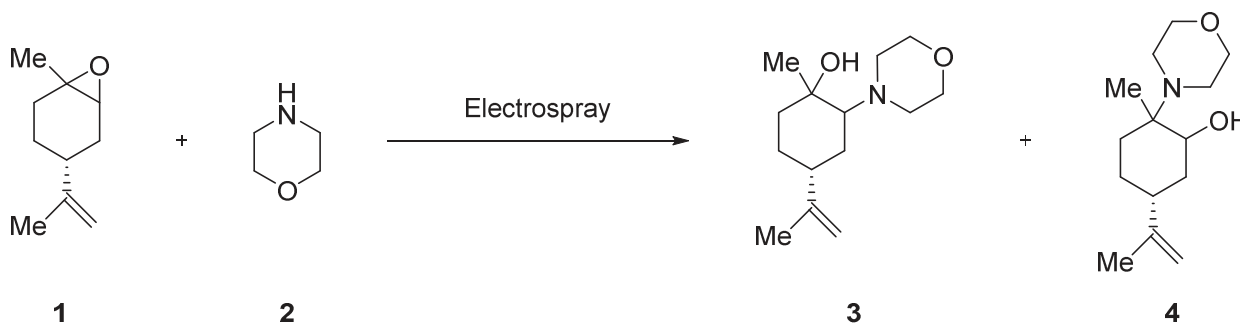


Figure 7: *ESI nebulizer coupled with mass spectrometer.*

Mass monitoring and kinetics acceleration

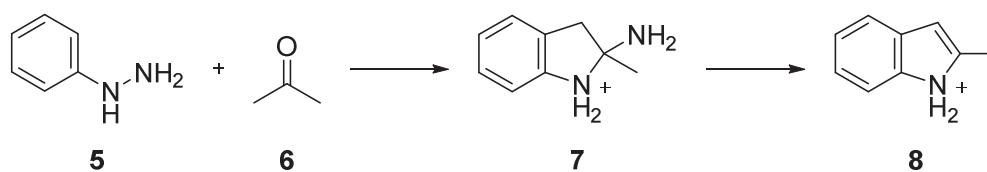
In the past few decades aerosol nebulization of reagents coupled with a mass analysis system was exploited to have a better understanding of reaction intermediates and reaction outcomes. Furthermore, another widely studied topic was the kinetic acceleration affecting nebulized reaction mixture in respect of bulk counterparts. For example Zare et al. performed nucleophilic ring opening of the limonene oxide (**1**) with morpholine (**2**) using an electrospray aerosol generator⁷.



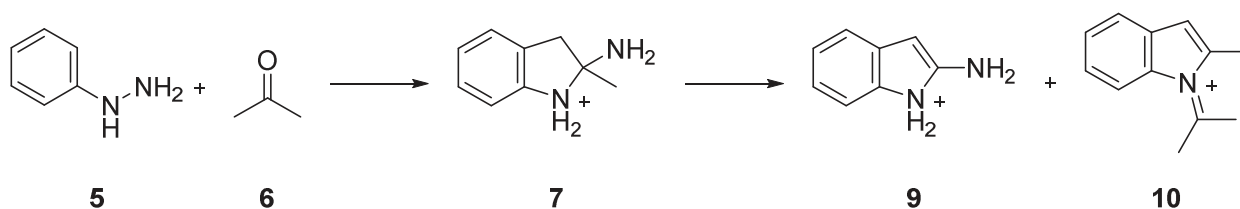
Reaction 1: *Nucleophilic opening of limonene oxide (**1**) with morpholine (**2**) to produce products (**3**) and (**4**).*

In bulk conditions and at room temperature, no products were detected after 90 min, while 2-3 μm diameters microdroplets of nebulized reaction mixtures afforded 0.5% product yield after 1 millisecond of flight time. This means that if we consider a 5% yield of the bulk reaction in 90 minutes the acceleration rate is about 105 times in the microdroplets environment.

Cooks et al. obtained a similar result showing an enhanced kinetics of a Fisher indole synthesis using. Also in this case, and electrospray ionization technique was adopted to generate microdroplets⁸.



Gas phase reaction



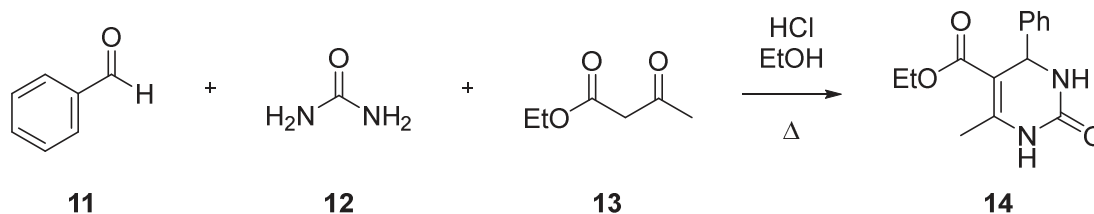
Microdroplets reaction

Reaction 2: Two routes by which phenylhydrazine (5) and acetone (6) react.

The study explored and compared gas phase and electrospray nebulizer generated aerosol reactions. Products obtained in the gas phase are reported in Reaction 2, together with those obtained in microdroplets without acetone excess (first step) and with acetone excess (second step). The collision induce dissociation that occurs when the reagents are present in their gas phase only gives a product (8) that is completely different from the one that occur as bulk phase under overnight reflux. Bulk phase and aerosol reaction afforded the same products (9), and no gas phase reaction product (8) is detected. With a modest acceleration factor of 10, the real breakthrough of this study deals with microdroplet lifetime effect. An increase of the distance between the needle and the charged surface in the EI setup, that correspond to an higher droplet lifetime, generated gas phase product (8). This happens because droplets dry out of the solvent allowing to react in a gas phase environment. The behaviour just described is something that as

to be always take into consideration while working with aerosol phase reactors.

Cooks et al. widely studied Biginelli reactions in a microdroplet environment⁹.



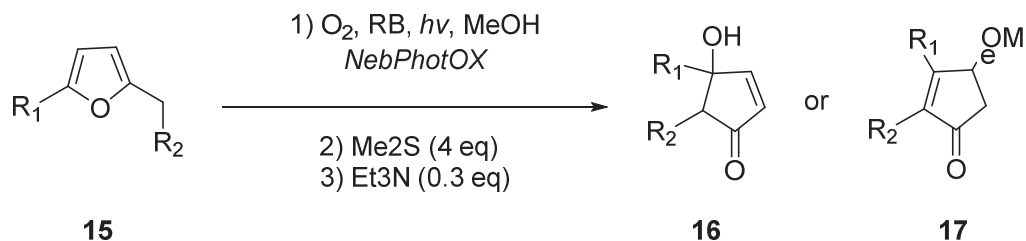
Reaction 3: *The condensation of benzaldehyde (11), urea (12) and ethyl acetoacetate (13) leading to the Biginelli synthesis of dihydropyrimidinones (14).*

This particular multicomponent reaction usually can proceed with a wide range of catalysts like Lewis acid, Brønsted acids, hydrogen bond donors and even transition metals. By the way just traces of the product is formed in bulk conditions over 48 hours with a catalyst-free approach. Cooks et. al. demonstrated that an aerosol reaction where microdroplets are generated via electrospray ionization could provide the desired product in the time range of milliseconds with, obviously, an enormous kinetic rate enhancement. Another novelty introduced by this work is the use of two separate barrels to generate droplets, the first dedicated to two reagents (11 and 13) and the second dedicated to the third reagent (12) nebulization. This method allows a better mixing of the reagents with product formation in μsec time scale. The authors explained that this relevant acceleration in the reaction rate presumably arises from the increased concentration of reagents during solvent evaporation in the microdroplet, reagent in confined space and change in the pH.

Aerosol reaction scaled up

Organic synthesis in aerosol phase with the analytical method of electrospray nebulization and the immediately analysis of the reaction outcome with mass spectroscopy techniques has some limits. The most important among them is the lack of reactions scale up: an improvement of the reaction kinetics is not enough in lab scale synthesis exploitation or, even worse, at an industrial production level. Electrospray nebulization can efficiently work only at nanoliters per minute liquid flow rates, paying also additional dilutions needs due to the high sensitivity of mass spectrometers¹⁰. For this reason, in the last 5 years, several scientific paper appeared in the

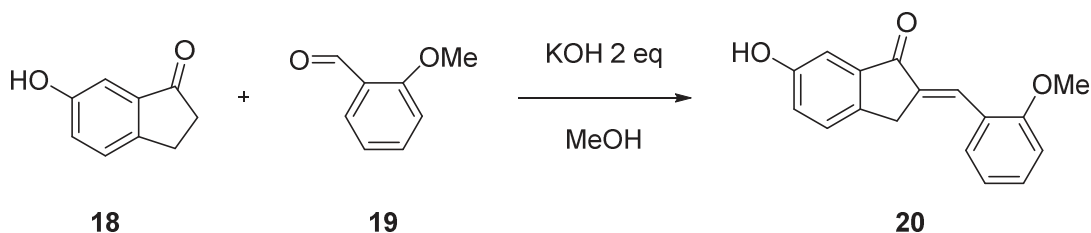
literature with the aim of increasing the reactors throughput developing the analytical method and using different nebulizers. For example, Vassilikogiannakis et al., presented a method for the synthesis of hydroxy- and methoxycyclopent-2-enones using a Burgener-like nebulizer and a condensation unit for the aerosol recovery at the end of the process¹¹.



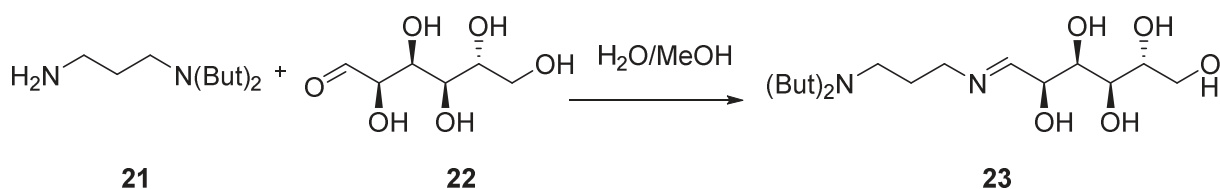
Reaction 4: *Piancatelli reaction: the synthesis of 4-hydroxycyclopent-2-enones 2 and 4-methoxycyclopent-2-enones 3 using the NebPhotOX system.*

This photochemical reaction exploited the use of singlet oxygen in situ generated by a proper LED strip, enabling an average final productivity of 0.5 mmol/min with excellent conversions.

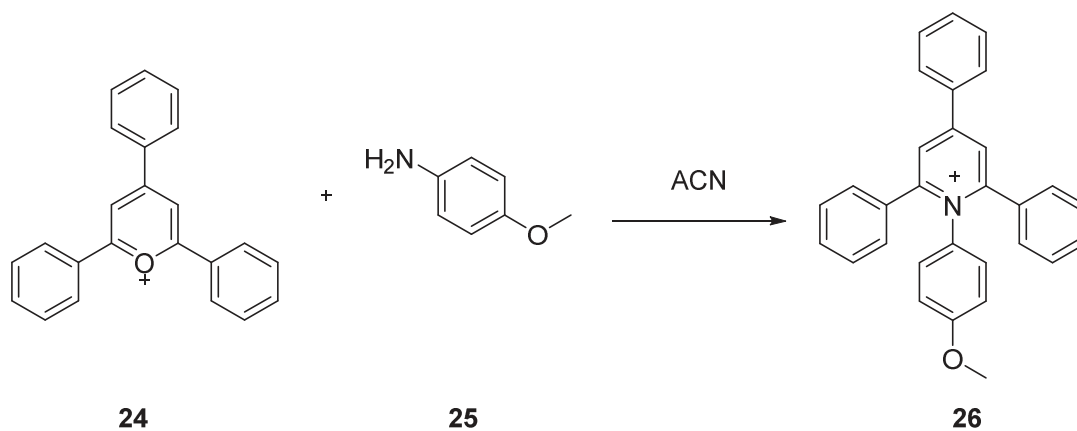
Also Cooks et al. worked with a variety of aerosol reactions in their scaled up versions¹². In this paper a continuous flow closed reactor was used to perform a Claisen-Schmidt reaction, a Schiff base reaction, a Katritzky reaction and a Suzuki reaction.



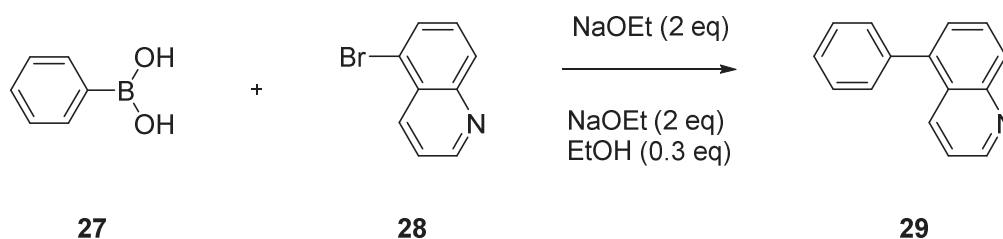
Reaction 5: *Base-catalysed Claisen-Schmidt reaction.*



Reaction 6: *Schiff base reaction.*



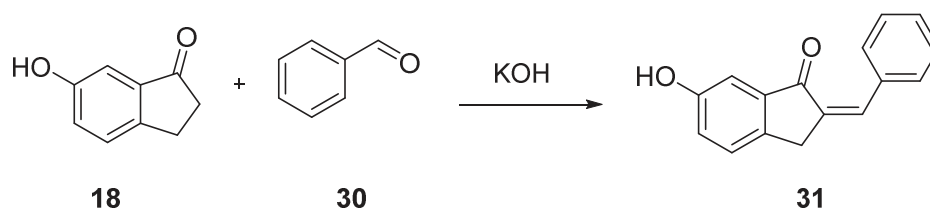
Reaction 7: *Katritzky reaction.*



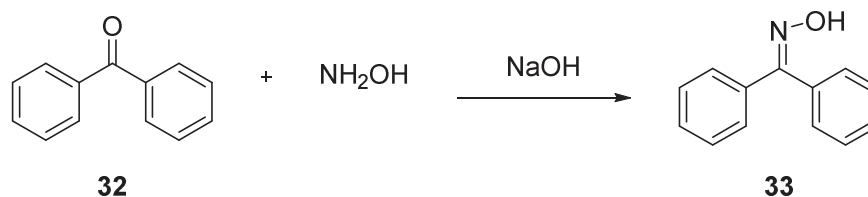
Reaction 8: *Suzuki reaction.*

Using a 10 mM concentrated reagent solution and a flowrate of 100 $\mu\text{L}/\text{min}$, an acceleration factor of 7700 times was achieved in the Claisen-Smith aerosol reaction compared to bulk conditions. The nebulizer was also provided with a micro and nanodroplets recycling facilities to ensure the complete mass recovery and yield between 72% and 100%. The following step was the scale up of the reaction and, for the Claisen-Smith reaction, the desired product was recover with 86.8% yield and up to 3,18 g/h productivity.

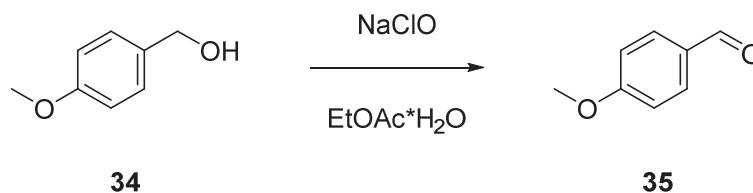
A completely different instrumental setup was instead used by Zare et al. to obtain the scale-up synthesis of a base-catalyzed Claisen-Smith condensation, an oximation reaction, a two phase reaction without the use of a phase transfer catalyst and an Eschenmoser coupling¹⁰.



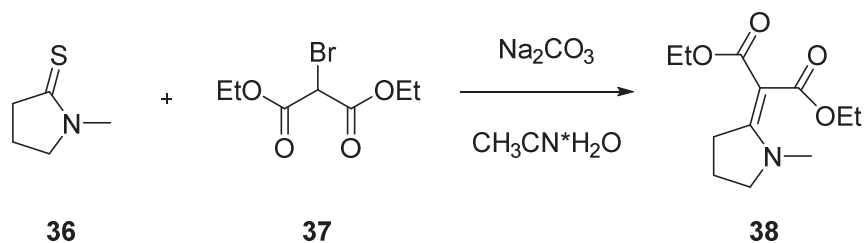
Reaction 9: *Base-catalysed Claisen-Schmidt reaction.*



Reaction 10: *Oximation reaction.*



Reaction 11: *Biphasic liq-liq oxidation reaction.*



Reaction 12: *Eschmoser coupling reaction.*

In this case a water bath ultrasound aerosol generator was used as nebulizer and the reactive solution in microdroplet phase was eventually heated inside a glass reactor through an heating tape. This setup enabled the reuse of the reactant solution indefinitely, avoiding the use of a condensation unit, but the reactor could not be considered as a continuous flow reactor. For

example the oximation reaction (**Reaction 10**) achieved an acceleration factor of 23 compared with the bulk phase reaction, with 21 mg/min productivity.

Very interesting was the case of a liq-liq biphasic reaction (**Reaction 11**), i.e. the reaction between immiscible reagents or reagents dissolved in immiscible solvents. An acceleration factor of 6536, with 31 mg/min productivity, was achieved in microdroplets compared to the corresponding bulk reaction. The acceleration of reaction rate can be largely assigned to an accumulation of reagents on the microdroplet surface^{13,14}. Particularly relevant in this case, is the complete absence of a phase transfer catalyst in the aerosol reaction, that is strictly required in the bulk immiscible biphasic liq-liq reaction.

Aim of the PhD

During three years of doctoral research my activity has been mainly focused on the development of novel aerosol reactors suitable for photochemical reactions and novel CCU methodological approaches exploiting carbon dioxide as reactive carrier-gas in aerosols. At the same time, working on this very novel topic required a strong engagement in the iterative design and implementation of equipment unavailable on the market. Regarding the photochemistry topic, the selective photooxidation of organic sulfides to the corresponding sulfoxide in aerosol via singlet oxygen has been performed, challenging the unprecedented exploitation of water and water/co-solvent selective sulfoxidation of organic substrates. In respect of the use of carbon dioxide as reactive-carrier gas, the research activity proceeded step by step in accordance with the following plan:

1. iterative design, implementation and test of a suitable aerosol reactor
2. identification of a suitable and effective catalyst to compare bulk and aerosol performances in respect of a model reaction
3. scope expansion of the identified reaction and process conditions to evaluate the robustness of the aerosol methodological approach.

References

1. Buglioni, L., Raymenants, F., Slattery, A., Zondag, S. D. A. & Noël, T. Technological Innovations in Photochemistry for Organic Synthesis: Flow Chemistry, High-Throughput Experimentation, Scale-up, and Photoelectrochemistry. *Chem. Rev.* (2021) doi:10.1021/acs.chemrev.1c00332.
2. Lévesque, F. & Seeberger, P. H. Highly efficient continuous flow reactions using singlet oxygen as a 'Green' reagent. *Org. Lett.* **13**, 5008–5011 (2011).
3. Heugebaert, T. S. A., Stevens, C. V. & Kappe, C. O. Singlet-oxygen oxidation of 5-hydroxymethylfurfural in continuous flow. *ChemSusChem* **8**, 1648–1651 (2015).
4. Raufaste, C., Bouret, Y. & Celestini, F. Reactive Leidenfrost droplets. *Epl* **114**, (2016).
5. Li, Y. *et al.* Accelerated Forced Degradation of Pharmaceuticals in Levitated Microdroplet Reactors. *Chem. - A Eur. J.* **24**, 7349–7353 (2018).
6. Bain, R. M., Pulliam, C. J., They, F. & Cooks, R. G. Accelerated Chemical Reactions and Organic Synthesis in Leidenfrost Droplets. *Angew. Chemie - Int. Ed.* **55**, 10478–10482 (2016).
7. Lai, Y. H., Sathyamoorthi, S., Bain, R. M. & Zare, R. N. Microdroplets Accelerate Ring Opening of Epoxides. *J. Am. Soc. Mass Spectrom.* **29**, 1036–1043 (2018).
8. Bain, R. M., Ayrton, S. T. & Cooks, R. G. Fischer Indole Synthesis in the Gas Phase, the Solution Phase, and at the Electrospray Droplet Interface. *J. Am. Soc. Mass Spectrom.* **28**, 1359–1364 (2017).
9. Sahota, N. *et al.* A microdroplet-accelerated Biginelli reaction: Mechanisms and separation of isomers using IMS-MS. *Chem. Sci.* **10**, 4822–4827 (2019).
10. Liu, C., Li, J., Chen, H. & Zare, R. N. Scale-up of microdroplet reactions by heated ultrasonic nebulization. *Chem. Sci.* **10**, 9367–9373 (2019).
11. Ioannou, G. I., Montagnon, T., Kalaitzakis, D., Pergantis, S. A. & Vassilikogiannakis, G. Synthesis of cyclopent-2-enones from furans using a nebulizer-based continuous flow

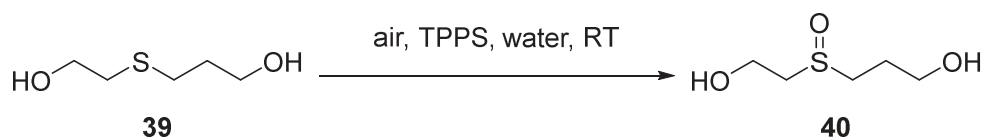
photoreactor. *Org. Biomol. Chem.* **15**, 10151–10155 (2017).

12. Nie, H. *et al.* High-yield gram-scale organic synthesis using accelerated microdroplet/thin film reactions with solvent recycling. *Chem. Sci.* **11**, 2356–2361 (2020).
13. Yan, X., Lai, Y. H. & Zare, R. N. Preparative microdroplet synthesis of carboxylic acids from aerobic oxidation of aldehydes. *Chem. Sci.* **9**, 5207–5211 (2018).
14. Mondal, S., Acharya, S., Biswas, R., Bagchi, B. & Zare, R. N. Enhancement of reaction rate in small-sized droplets: A combined analytical and simulation study. *J. Chem. Phys.* **148**, (2018).

Design and manufacture of novel reactors

Photochemical reactors

While approaching the first aerosol reaction, emerged the need of designing and build a simple and cheap photoreactor with some specific features. It was tailored to test our model photochemical reaction (Scheme 1) in aerosol mode, monitoring starting materials conversions and reaction selectivity.



Reaction 8: *Identified model photochemical reaction.*

Accordingly, a plastic medical nebulizer was customized and fit with a glass colorless tube (8 cm length, total volume 32 mL), suitably adapted from unused laboratory glassware. This handcrafted prototype was equipped with an *ad hoc* made condensing unit (a plastic pipette tip, slightly widened to avoid any back-pressure, placed within a water filled 10 mL vial) depicted in Figure 8. Before testing the system, the pre-fitted nebulizer and the post-adapted condensing units were darkened with aluminum foils and black tapes to avoid any undesired reagents' photochemical conversion. Only the central glass tube was irradiated by suitable lamps, exposing to light sources for photochemical reaction only microdroplets passing through the transparent tube.

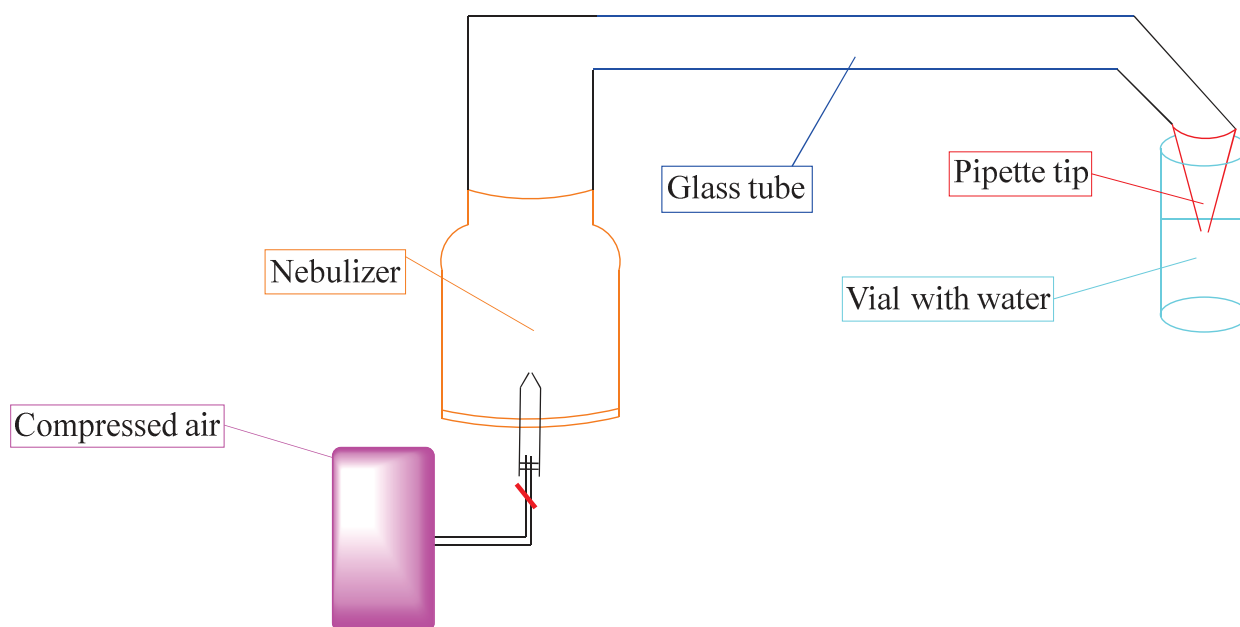


Figure 8: Representative scheme of the first nebulizer used.

This device revealed several issues:

1. insufficiently long, resulting in an inadequate microdroplets lifetime for oxidation completion at the adopted gas flowrate (750mL/min);
2. a better assembly of modules was required to avoid any reagent loss throughout the reactor;
3. the unsatisfactory mass recovery through the final condensing unit threatened the final yield of the whole reaction and processing operations.

Based on these evidences, a glass nebulizer was adopted instead of the plastic counterpart, and a longer glass tube (57,2 cm length, 115 mL volume) replaced the shorter previously tested, in this way also facilitating tight connections among reactor's modules. Particular attention was paid to the glass tube geometry. To avoid any unproductive light decay, a long tube with minimized inner diameter ($\phi_{in} = 16$ mm) was preferred, since the light intensity decays with the square root of the distance from the light source.

Finally, alternative condensing units were tested, and the identified best performing condensation system resembled that reported in the literature,¹⁵⁻¹⁷ although a second condensation step was not arrayed to the first one. In our case, the adopted solution consisted of

a cooled and opened Schlenk flask, filled with water, equipped with a small tube (connected at the bottom of the light exposed glass unit) finally immersed therein and, where the collected aerosol was bubbled and condensed (Figure 9).

At the beginning just one lamp was installed under the glass tube but soon 4 more lamp were added all around the glass tube to increase the total light intensity and to ensure that all the part of the reactor were homogeneously irradiated.

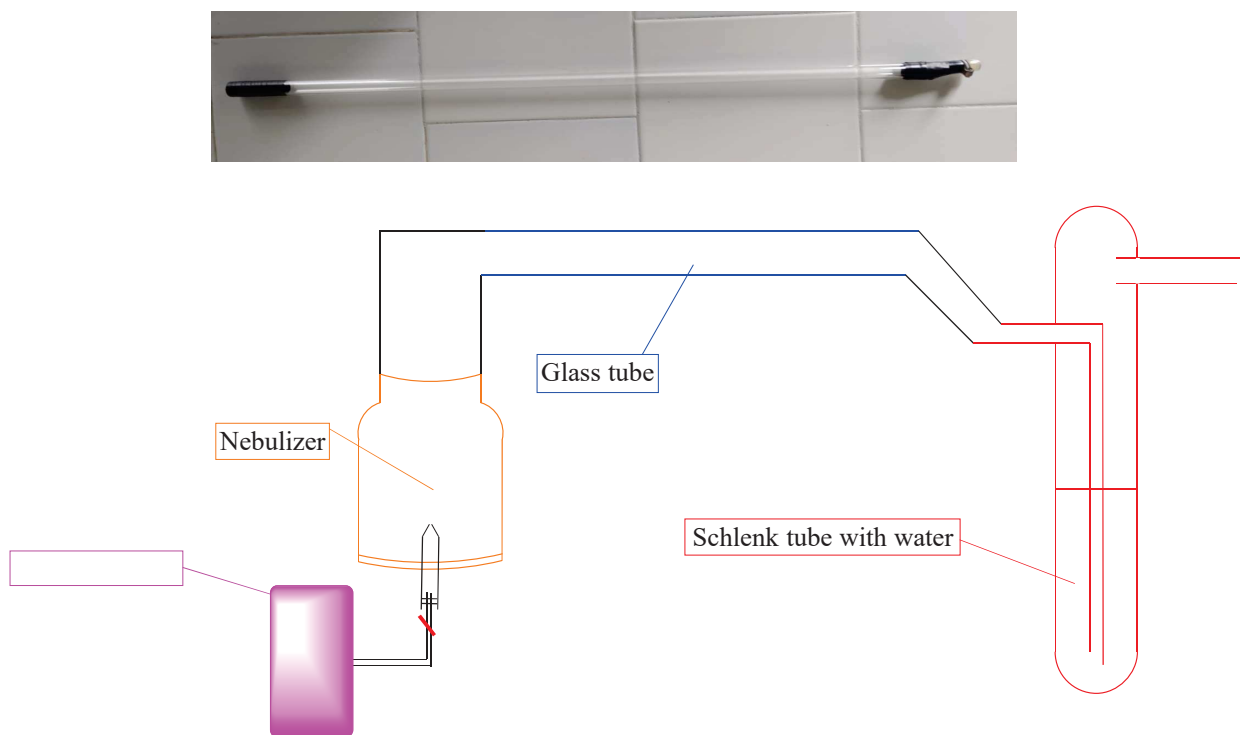


Figure 9: *The glass tube used in the second reactor and its representative scheme.*

Through a fruitful and intense collaboration with the University of Leuven (KULeuven), especially with associate professor Mumin Enis Leblebici, a lab scale photoreactor (Figure 10) was finally realized, suitably shaped for the photooxidation of a water soluble sulfide via singlet oxygen¹⁸.

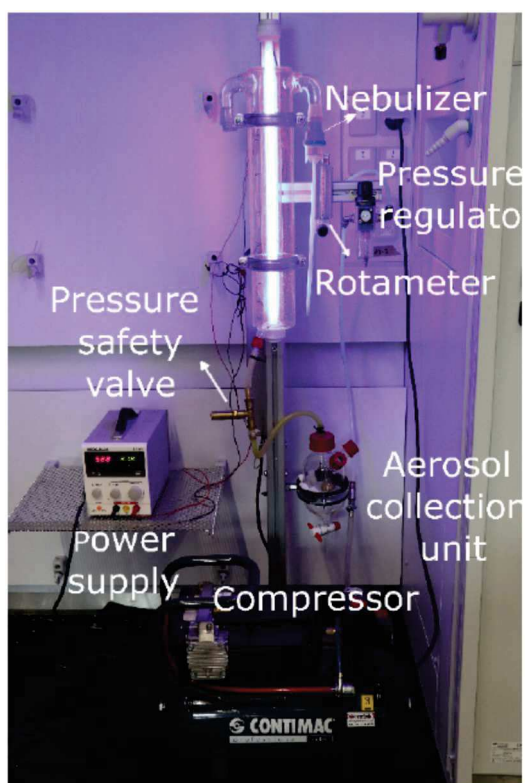


Figure 10: Picture of the lab scale photoreactor in action.

The 1860 mL total volume photoreactor was built and used in the laboratory of Diepenbeek campus (Belgium). This particular reactor was equipped with a plastic medical nebulizer directly attached to an air compressor.

Trough an air back pressure regulator, the operating reactor air pressure was adjustable up to 3 bar, and the air flowrate was regulated with a rotameter installed on the air feed line.

Even if the reactor operating pressure can be adjusted up to the pre-set limit, the reactor always operated at atmospheric pressure, limiting any safety issue leaving the reactor opened to the air to avoid pressure building-up.

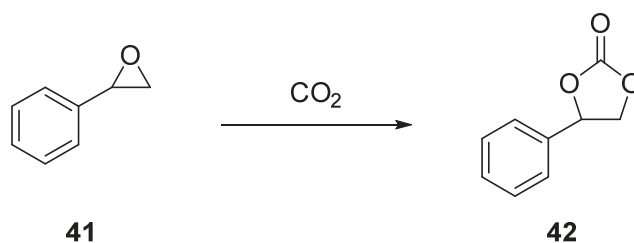
The aerosol back condensation unit of this final reactor consisted of a glass frit inserted in a modified separation funnel; an extra hole was drilled in the funnel to keep the overall pressure at atmospheric level. Relevant and innovative feature of this custom made photoreactor is its annular geometry, that placed the light source in the central hole, also called the annular region^{19,20}.

Carbon dioxide utilization reactors

The implementation of a suitable reactor for reactive aerosols generated using carbon dioxide as a carrier and reactive gas should take into account several issues, even at the initial design stage. These issues can be summarized as follows:

1. the intrinsic CO₂ chemical stability requires the development of catalyzed reactions to overcome the consequently high activation energies;
2. longer microdroplets average lifetime should be considered in respect of the abovementioned fast photo-oxidations;
3. since no CO₂ photochemical reactions are considered in this thesis, a simpler aerosol reactor should be designed in respect of the annular prototype implemented above for the selective sulfide photo-oxidations.

With all these constraint and opportunities clearly identified, also in this case a step-by-step approach to the design and implementation of a suitable CO₂ aerosol reactor have been followed. The identified model reaction is represented in Reaction 9.



Reaction 9: *Identified CO₂ model reaction.*

Accordingly, an initial and rudimental handcrafted 3L flow reactor was built using two 1.5 L plastic bottles, cut on the bottom, and front-to-front attached each other. This system, characterized by an unsatisfactory mass recovery and the end of the process, the microdroplet average lifetime (corresponding to the residence time) was suitable extended to appreciate a low, but encouraging, starting materials conversion.

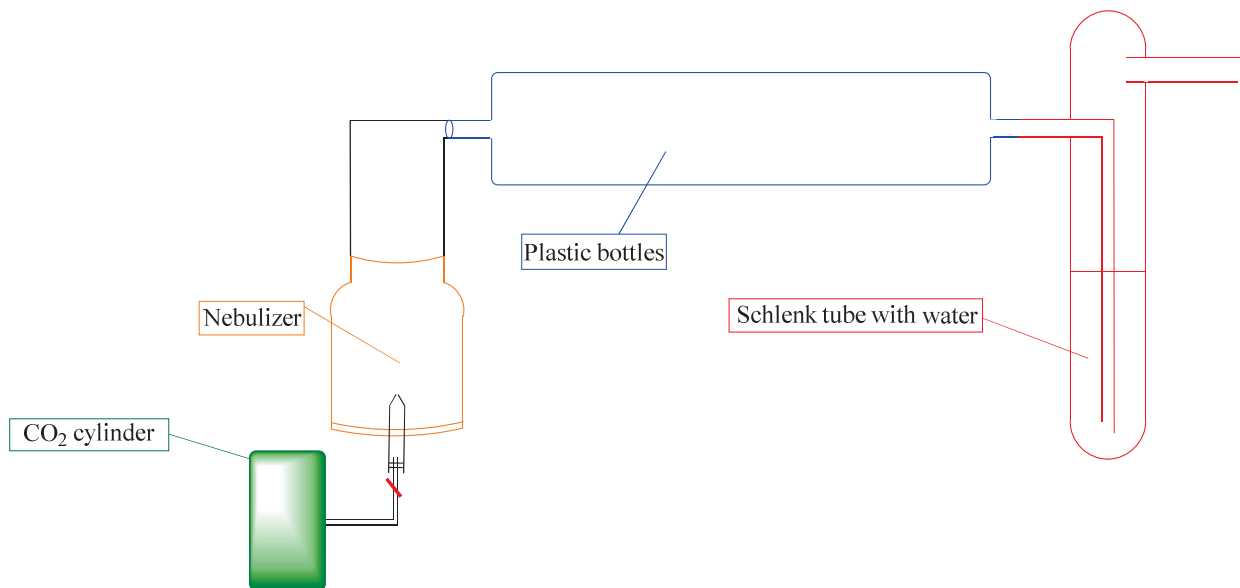


Figure 11: *Plastic bottles used as reactor chamber and reactor representative scheme.*

Despite significant improvements of the initial reactor design were stepwise achieved, clearly emerged the need to move from a flow to a batch reactor, in which the reactive solution was continuously nebulized inside a CO₂ filled close vessel. The new batch reactor was implemented using a 2L separation funnel, adapting a polypropylene plastic cup on the funnel neck as a ultrasonic transparent membrane (Figure12). To generate the aerosol fountain, the separation funnel was reversed upside down, and the polypropylene plastic cup was exposed to the piezoelectric transducer immersed in the water bath of an ultrasonic water bath nebulizer available on the market, adapted to our needs before starting the methodological exploration.

The separation funnel was selected because allowed:

1. a closed reactor during the reaction (no aerosol leaking through the tap)
2. o vacuum-CO₂ cycles to ensure a final CO₂ environment at atmospheric pressure.



Figure 12: *Picture of the batch aerosol reactor during a reaction.*

By the way several problem arose since the beginning:

1. low mechanical resistance of the cup that usually broke during vacuum cycles;
2. air bubbles under the cup (inside the water bath) stopped ultrasonic transmission and should be carefully removed;
3. high viscous liquids didn't nebulize because of inadequate nebulizer power.

To solve those problems several changes in the reactor design were made.

The plastic cup was replaced by a thin aluminum foil, blocked on the separation funnel neck through a plastic screw cap drilled in the center. This setup allowed vacuum-CO₂ cycles and avoided any leaking of the reagents in the water bath.

Air bubbles between the aluminum foil and the water bath still challenged the system operations, but tilting and moving the water bath immersed reactor from the vertical position mitigate the problem. Reagents viscosity remained an issue with this setup, and dilution with a suitable

cosolvent should be considered to allow nebulization. By the way, one of the limit of this batch aerosol approach was still evident and has to be properly discussed.

Upon switching on the nebulizer, only a fraction of the reaction solution is nebulized, enjoying all microdroplets advantages discussed in the previous chapter. Along with the generated aerosol, a significative amount of reaction solution still remain in the liquid bulk. This generates a kind of equilibrium between microdroplets and the bulk phase, allowing the first to back-condenses into the liquid bulk, and this latter to nebulize. Reagent conversion proceed faster in the aerosol phase than in the bulk, and an acceleration factor calculated with reaction composition data retrieved from the liquid bulk analysis is inherently underestimated and should be consider only an apparent measure. The apparent acceleration factor depends on the microdroplets/liquid bulk ratio: the more liquid in microdroplets the greater the apparent acceleration factor will be.

Therefore a flow-like reactor seems to be an improvement of the batch reactor just described. In this newly designed reactor a small nebulizer, equipped with the aluminum foil and the plastic screw cap, is directly connected to a big flask where only microdroplets should be able to move (Figure 13).

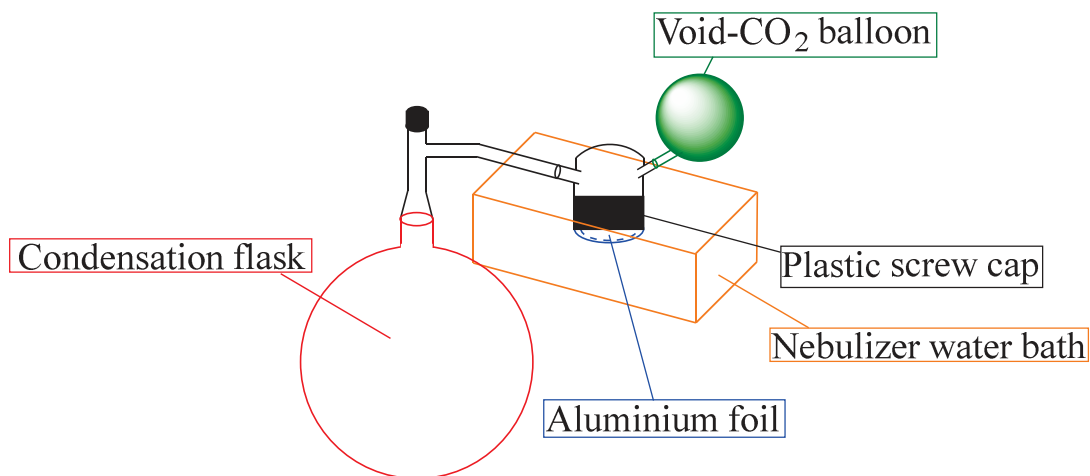


Figure 13: *Flow-like aerosol reactor.*

The principal idea of this newly built reactor is the fact that moving the microdroplets generated into another area will form a non-equilibrium condition and so, to return to a state of equilibrium, more liquid from the bulk phase should be nebulized. Even if the aim of this reactor is to “move”

microdroplets from the nebulizer to the collector flask, this reactor cannot be considered as a flow reactor because the whole system is closed and there is no gas inlet flow. As in previous case the CO₂ atmosphere is obtained through vacuum-CO₂ cycles. Unfortunately this reactor did not match the expected result. Aerosol mist behave more like a liquid than a gas, even if the microdroplets tries to separate themselves from each other to occupy all the available space, they are really sensitive to the gravitational field and place themselves in a vertical gradient: close to the bulk phase there are a lot of microdroplets that slowly decrease moving away from the nebulizer and rising in height. This particular behavior was the main limit which prevented the flow-like reactor from working properly as too few microdroplets pass from the nebulizer to the collection flask.

Modular reactor for aerosol synthesis

A modular glass reactor was designed and custom made to overcome all above difficulties, met while working with CO₂ as a carrier and reactive gas in flow regime. This modular reactor consist in several components that can be installed in various arrangements to run different kind of reactions. Like other setups, also in this case is possible to divide the reactor in three part: the nebulizer, the main core where the reaction takes place and the condensation unit.

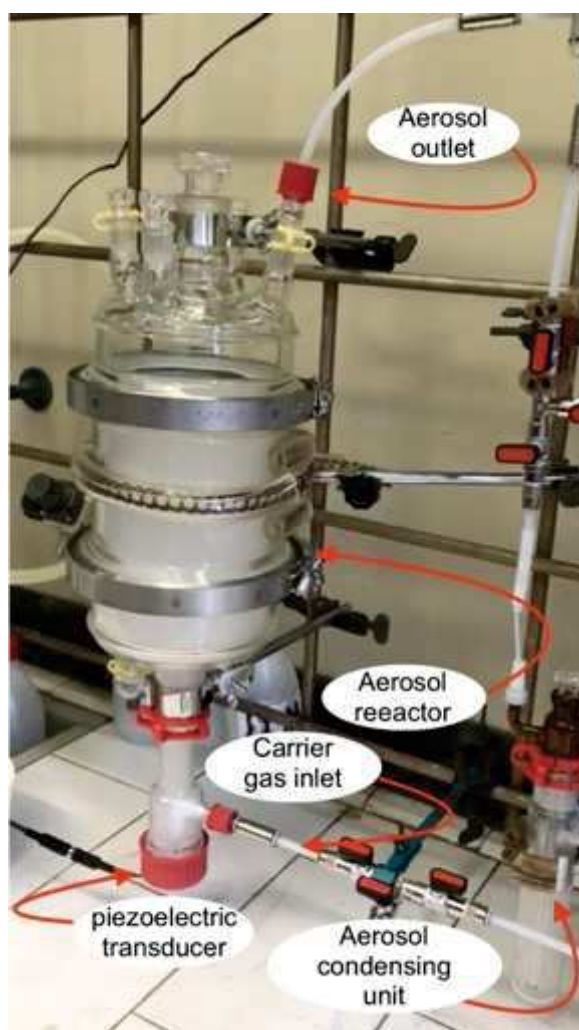


Figure 14: Custom-made modular reactor for aerosol synthesis.

Regarding the nebulizer, various options can be adopted. The modular reactor is compatible with the classical glass medical nebulizer that can be used to spray a solution from the top of the reactor. Through the use of a thermostatic oil bath is also possible to keep the medical nebulizer at a constant temperature to avoid precipitation of the reagents due to temperature drop. Ultrasonic nebulizers can be used in two different way: the first one is from the bottom of the reactor in batch conditions as it was used previously, the second one consist in the use of the piezoelectric transducer on its own without the water bath mediation (Figure 15). For the second case a new nebulizer was purchased and consist in a chamber with a screw cap on the bottom where the piezoelectric transducer can be attached and, on a side, an opening that gives the possibility of feeding the nebulizer with a carrier or reactive gas, in our case CO₂, with consistent

flow rate. This nebulizer can be used indifferently to nebulize a solution from the top or for the bottom of the reactor.

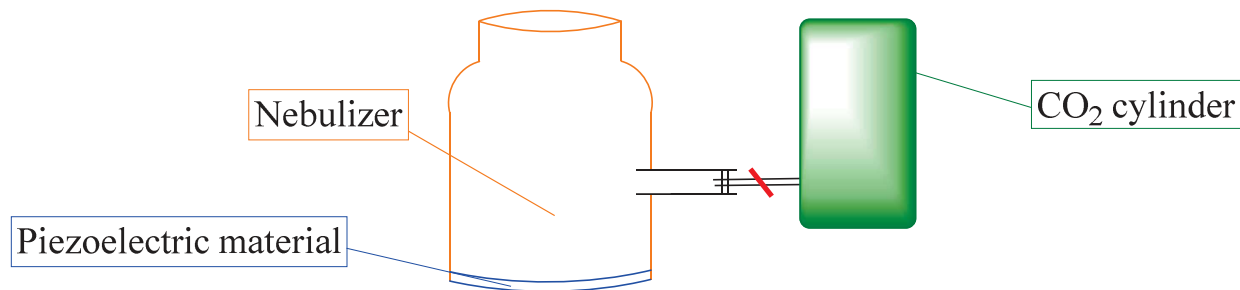


Figure 15: Home-build ultrasonic nebulizer.

The main core of the modular reactor consists of three different parts: two lids with different kind of opening on top of them and a central part that separate them. The central part is just a cylinder of glass with a pre-determined height that can be changed to stretch the microdroplets average lifetime if needed. The lids are similar to the ones used for dryers and are fitted with a flange and a seal to be firmly attached to the glass cylinder. Several opening are present on top of the lids to give to possibility to attach nebulizer and condensation unit but also other instrument like thermocouples, stirring devices and so on.

The condensation unit in this case is similar that proposed by Vassilikogiannakis et. al¹⁵⁻¹⁷. The modular reactor was equipped with two different Schlenk flask arrayed and cooled with an ice and salt baths. Finally, a cooled round bottom flask was installed to enhance the condensation efficiency of the modular reactor.

A LEDs holder was than designed and custom-made to allow the use of this modular reactor for photochemical aerosol reactions. This LEDs holder consist in a wide cylinder that can be placed inside the reactor, equipped with a smaller tube that can reach the top or the bottom of the main core to allow electric connections of lamps placed therein and to be blocked inside the reactor. This opening is also useful to introduce a constant air flow to reduce the LEDs temperature and avoid lights damages. On the opposite part, a glass tap is used to avoid any aerosol leaking through the LEDs area. The LEDs are mounted on a small rectangular steel stand that allows 4 different LEDs to be positioned simultaneously and easily interchanged with other LEDs if required.

References

15. Pergantis, S. A., Montagnon, T., Vassilikogiannakis, G., Kalaitzakis, D. & Ioannou, G. I. A Novel Nebulizer-Based Continuous Flow Reactor: Introducing the Use of Pneumatically Generated Aerosols for Highly Productive Photooxidations. *ChemPhotoChem* **1**, 173–177 (2017).
16. Ioannou, G. I., Montagnon, T., Kalaitzakis, D., Pergantis, S. A. & Vassilikogiannakis, G. Synthesis of cyclopent-2-enones from furans using a nebulizer-based continuous flow photoreactor. *Org. Biomol. Chem.* **15**, 10151–10155 (2017).
17. Ioannou, G. I., Montagnon, T., Kalaitzakis, D., Pergantis, S. A. & Vassilikogiannakis, G. One-Pot Synthesis of Diverse γ -Lactam Scaffolds Facilitated by a Nebulizer-Based Continuous Flow Photoreactor. *ChemPhotoChem* **2**, 860–864 (2018).
18. Kayahan, E. *et al.* Overcoming mass and photon transfer limitations in a scalable reactor: Oxidation in an aerosol photoreactor. *Chem. Eng. J.* **408**, 127357 (2021).
19. Boiarkina, I., Norris, S. & Patterson, D. A. The case for the photocatalytic spinning disc reactor as a process intensification technology: Comparison to an annular reactor for the degradation of methylene blue. *Chem. Eng. J.* **225**, 752–765 (2013).
20. Lim, T. H. & Kim, S. D. Trichloroethylene degradation by photocatalysis in annular flow and annulus fluidized bed photoreactors. *Chemosphere* **54**, 305–312 (2004).

Photochemical reactions in bulk condition

Singlet oxygen and previous studies

Singlet oxygen ($^1\text{O}_2$), the first excited state of molecular oxygen ($^1\Delta_g$)²¹ is an important reagent used in medicinal chemistry^{22,23} and organic synthesis, due to its reactivity and environmental benign features²⁴. The oxygen molecule is characterized by a triplet ground state ($^3\text{O}_2$), and the lowest excited state is a singlet state that can be populated by energy transfer through many excited molecules acting as photosensitizers as per the following reactions:

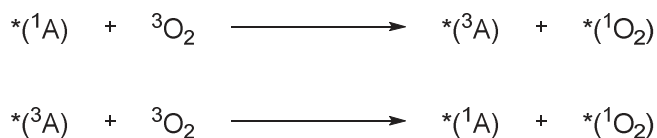


Figure 16: *Different ways to populate singlet oxygen excited state.*

Both reactions are spin allowed, the first takes place between the two species, when the singlet-triplet energy gap of A is bigger than the energy gap between triplet-singlet energy gap of molecular oxygen, the second one has just one-ninth of probability to have the overall singlet multiplicity for both species. The general trend in photochemistry is that an excited molecule is always a better oxidant or a better reductant than the corresponding ground state counterpart, and this is also true for oxygen²⁵.

Therefore the easiest way to produce singlet oxygen is to generate it in situ by dye-sensitized energy transfer method²⁶. Nevertheless singlet oxygen can also be prepared from the decomposition of compounds like triethylsilyl hydrotrioxide²⁷ and phosphite ozonides²⁸. Typical organic chemistry reactions exploiting singlet oxygen are: the Diels-Alder [4+2] and [2+2]-cycloaddition²⁹. Singlet oxygen is well known for its use in diastereoselective syntheses³⁰, the oxidation of amines³¹, phosphines³² and sulfides³³.

The aim of this part of my research activity was the selective water photo-oxidation of organic sulfides to the corresponding sulfoxides mediated by a suitable photosensitizer. In this case 5,10,15,20-Tetraphenyl-21H,23H-porphine-p,p',p,p''-tetrasulfonic acid tetrasodium hydrate

(TPPS, Figure 17) has been selected and tested, due to its maximum light absorption at $\lambda = 418$ nm (Soret band), and its high solubility in water.

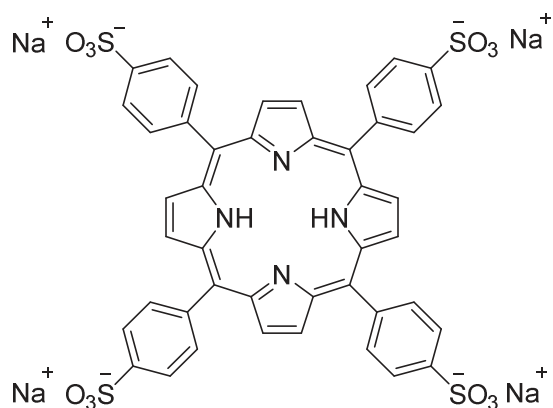


Figure 17: TPPS structure.

TPPS is a derivative of the more common tetraphenylporphyrin (TPP), that has been sulfonated without any significant loss in photocatalytic activity. The necessity of being able to have a photosensitizer soluble in water comes from the fact that singlet oxygen lifetime is lower in water than in other common organic solvents³⁴.

Sulfoxides are key moieties in APIs (omeprazole and omeprazole-like compounds) and in broad-spectrum insecticides like the phenylpyrazoles chemical family (Fipronil), Figure 18.

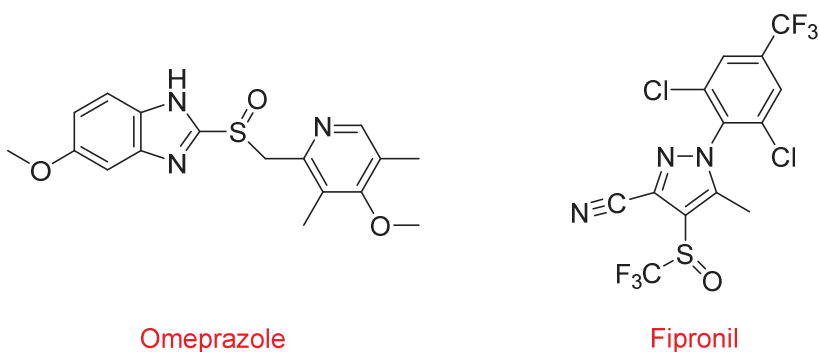
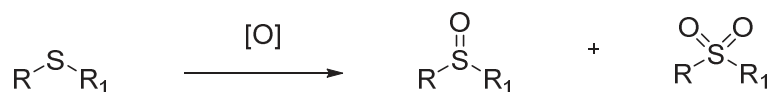


Figure 18: Relevant bioactive sulfoxides.

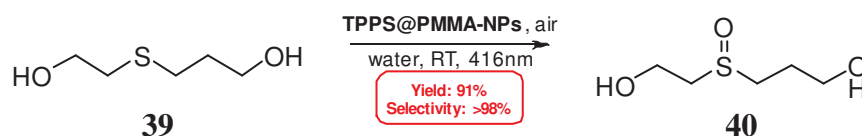
Sulfoxides are typically prepared using hydrogen peroxide³⁵ through expensive and toxic metal complexes catalysed reactions. Furthermore, the selective oxidation of sulfides to sulfoxides is a challenging reaction due to the overoxidation to sulfones in common organic solvents²⁴ (Reaction 10).



Reaction 10: General sulfide oxidation scheme, highlighting the selectivity issue.

Therefore, a green and feasible procedure is needed to provide the selective synthesis of a wide spectrum of organic sulfoxides.

In a previous paper of the group in which I have worked³⁶, the water soluble model sulfide **39** was selectively photo-oxidized to the corresponding sulfoxide **40** through an efficient in-water continuous-flow procedure (91% isolated yield, selectivity over 98%), Reaction 11.



Reaction 11: Selective photo-oxidation of a model sulfide.

The abovementioned procedure mainly suffers of scalability issues. On the other hand, organic sulfoxides can be easily separated from the water soluble photosensitizer. Accordingly, the first step of this project was to provide an innovative organic sulfides oxidation methodology, using ethanol as a green co-solvent and TPPS as a photosensitizer.

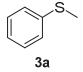
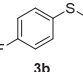
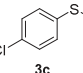
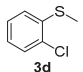
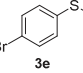
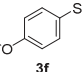
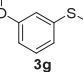
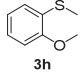
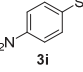
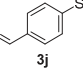
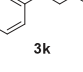
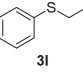
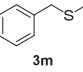
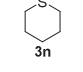
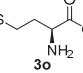
Bulk photochemical oxidation of organic sulfides with water

Solubility studies

Among the known organic sulfides, only a very limited fraction of them are water soluble. In order to transfer the bulk optimized procedures to aerosol reactions, in which homogeneous solutions are initially required to study simple reacting systems, a suitable solvent mixtures affording homogeneous solutions were explored. Ethanol/water mixtures were chosen as green co-solvents, since ethanol is completely miscible with water and keeps the singlet oxygen lifetime at an acceptable level¹³. The complete solubility of each organic sulfides in an ethanol/water mixture was confirmed through UV-vis spectroscopy. The proper solvents ratio

was identified case-by-case, through stepwise additions of water (until precipitation), to homogeneous ethanol sulfide solutions. Accordingly, scattering phenomena were monitored at 640 nm (no sulfides absorption detected at that wavelength) on 0.1 M solution of each sulfide. The solubility limit was identified when the absorbance difference between the sample and the reference solution exceeded 0.2 Abs, corresponding to light scattering onset assigned to undissolved sulfides. In Table 1, ethanol/water ratio are case-by-case reported.

Table 1: Organic sulfides solubility data in ethanol/water mixtures.

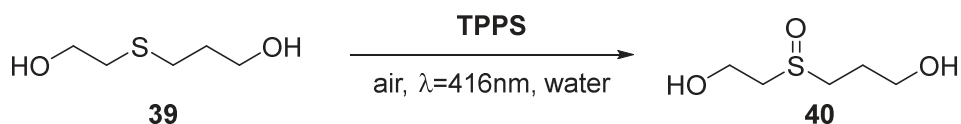
SULFIDE	SOLVENT	SOLVENT RATIO	CONCENTRATION (M)	VALUE (Abs*100)	WAVELENGTH (nm)	
 3a	Thioanisole	EtOH/H ₂ O	1:1	0.1	-0.56	640
		EtOH/H ₂ O	1:3	0.1	187.28	640
 3b	4-fluoro thioanisole	EtOH/H ₂ O	1:1	0.1	0.41	640
		EtOH/H ₂ O	1:3	0.1	103.16	640
 3c	4-chloro thioanisole	EtOH/H ₂ O	3:1	0.1	-0.40	640
		EtOH/H ₂ O	1:1	0.1	114.37	640
 3d	2-chloro thioanisole	EtOH/H ₂ O	3:1	0.1	-0.27	640
		EtOH/H ₂ O	1:1	0.1	201.04	640
 3e	4-bromo thioanisole	EtOH/H ₂ O	9:1	0.1	0.91	640
		EtOH/H ₂ O	3:1	0.1	preprecipitated visible	640
 3f	4-methoxy thioanisole	EtOH/H ₂ O	3:1	0.1	-0.37	640
		EtOH/H ₂ O	1:1	0.1	4.99	640
 3g	3-methoxy thioanisole	EtOH/H ₂ O	3:1	0.1	-0.10	640
		EtOH/H ₂ O	1:1	0.1	4.21	640
 3h	2-methoxy thioanisole	EtOH/H ₂ O	3:1	0.1	-0.78	640
		EtOH/H ₂ O	1:1	0.1	52.82	640
 3i	4-nitro thioanisole	EtOH	/	0.1	49.03	640
		CH ₃ CN	/	0.1	0.08	640
 3j	4-methylthio benzaldehyde	EtOH/H ₂ O	3:1	0.1	0.04	640
		EtOH/H ₂ O	1:1	0.1	50.54	640
 3k	allyl phenyl sulfide	EtOH/H ₂ O	3:1	0.1	0.75	640
		EtOH/H ₂ O	1:1	0.1	147.40	640
 3l	ethyl phenyl sulfide	EtOH/H ₂ O	3:1	0.1	0.02	640
		EtOH/H ₂ O	1:1	0.1	31.04	640
 3m	benzyl methyl sulfide	EtOH/H ₂ O	3:1	0.1	-0.39	640
		EtOH/H ₂ O	1:1	0.1	13.91	640
 3n	pentamethylene sulfide	EtOH/H ₂ O	1:1	0.1	0.11	640
		EtOH/H ₂ O	1:3	0.1	4.66	640
 3o	L-methionine	H ₂ O	/	0.1	0.08	640

Result and discussion

With the aim of selecting the optimal sulfide/TPPS concentration ratio that gives a fast and complete oxidation, a preliminary investigation (Table 2) of the model photooxidation was attempted in water with the model sulfide **39**.

Table 2. Comparison between the concentration of starting sulfide and TPPS.^a

Table 2: Comparison between the concentration of starting sulfide **39** and TPPS^a.



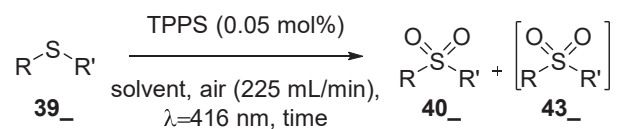
ENTRY	TIME (min)	[SULFIDE] (M)	[TPPS] (M)	CONVERSION (%) ^b
1	90	0.1	5*10 ⁻⁵	>99.5
2	90	0.1	5*10 ⁻⁶	94.5
3	120	0.1	5*10 ⁻⁷	93.9

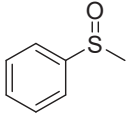
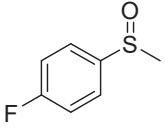
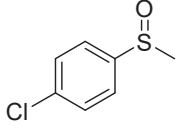
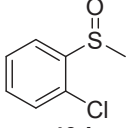
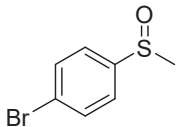
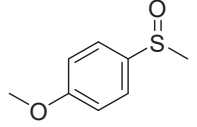
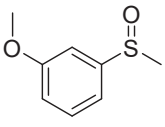
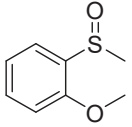
^a**1** (0.2 mmol), sonicated water (2 mL), air flow 225 mL/min, $\lambda=416$ nm. ^bConversion determined by qNMR.

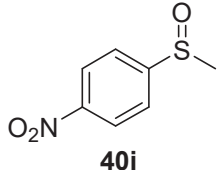
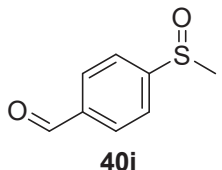
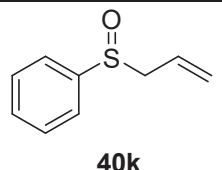
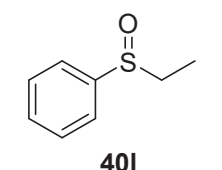
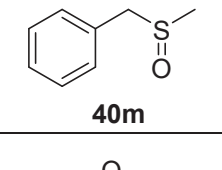
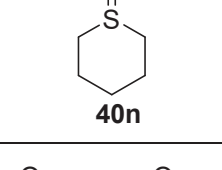
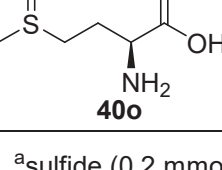
Even though high conversion was obtained using TPPS concentration as low as 5*10⁻⁷ M (Entry 3, Table 1), it was decided to use an higher ratio of TPPS:sulfide (Entry 1, Table 2) in order to have fast and reliable experiments.

Having identified the optimal reaction conditions (Table 2, entry 1) and the solubility limits of each sulfide in EtOH/H₂O the solvent mixture (Table 1), a wide range of organic sulfides were photo-oxidized accordingly. Table 3 summarized the exploration outcome.

Table 3: Scope expansion organic sulfides^a.



ENTRY	SULFOXIDE	EtOH:H ₂ O	TIME (min)	CONVERSION (%) ^b	SULFONE (%) ^b	ISOLATED YIELD (%) ^c
1	 40a	1:1	90	>99.5	ND	86
2	 40b	1:1	90	>99.5	ND	90
3	 40c	3:1	120	>99.5	ND	91
4	 40d	3:1	120	63.9	ND	55
5	 40e	9:1	120	90.1	ND	78
6	 40f	3:1	120	94.3	ND	83
7	 40g	3:1	120	99.2	ND	86
8	 40h	3:1	120	99.4	ND	81

9		CH ₃ CN	120	/	/	/
10		1:1	120	99.4	ND	95
11		3:1	120	>99.5	3.4	88
12		3:1	120	>99.5	7.4	70
13		3:1	90	>99.5	0.6	72
14		1:1	90	>99.5	ND	78
15		H ₂ O	90	97.1	ND	65 ^d

^asulfide (0.2 mmol), TPPS (1*10⁻⁴ mmol), air flow fixed at 225 mL/min, radiant flux fixed at 10 mW.

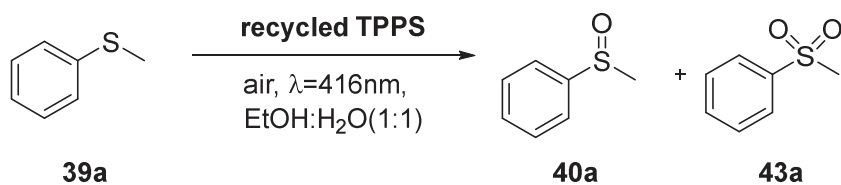
^bDetermined by ¹H qNMR technique. ^cAfter extraction with Me-THF and chromatography.

^dAfter 24h of liofilization.

Fortunately, thioanisole (**39a**) was oxidized to the corresponding sulfoxide (**40a**) as the model sulfide, with high conversion and selectivity (Table 3, Entry 1). This important result confirmed that the presence of ethanol in the reaction mixture didn't affect TPPS reactivity. Same result was obtained with 4-fluorothioanisole (**39b**) (Table 3, Entry 2), however the other *para*-halogenated sulfides required longer reaction time to reach almost complete conversions and

full selectivity (Table 3, Entry 4 and 5). In the case of 2-chlorothioanisole (**39c**) (Table 3, Entry 3) a conversion of 63.9% was obtained after 120 min, probably due to steric hinderance of the heteroatom. In the case of the methoxy-thioanisole compounds (**39f,g,h**) the different position of the substituent on the aromatic ring didn't affect the oxidation and selectivity (Table 3, Entry 6,7 and 8). As expected, the oxidation of the high electron poor 4-nitrothianisole (**39i**) was not happening probably due to the low reactivity of the substrate (Table 3, Entry 9). The aldehyde moiety of 4-methylthiobenzaldehyde (**39j**) was not oxidize by the singlet oxygen to the corresponding carboxylic acid. Instead this sulfide reached almost complete conversion and selectivity (Table 3, Entry 10). Allyl phenyl sulfide (**39k**) was completely converted into the corresponding sulfoxide (**40k**) although traces of the corresponding sulfone were detected (**43k**) (Table 3, Entry 11). Also the ethyl phenyl sulfide (**39l**) showed riduced selectivity, with 7.4% of detected sulfone (**43l**) (Table 3, entry 12). The benzyl methyl sulfide (**39m**) was completely oxidized, showing negligible amount of the corresponding sulfone (**43m**) (Table 3, Entry 13). Also for aliphatic sulfide singlet oxygen photooxidation was explored. Almost complete and selective oxidation of pentamethylene sulfide (**39n**) is reported in Table 3, Entry 14. Finally, L-methionine (**39o**) was oxidized in pure water, showing a very good conversion and no traces of the corresponding by-product (Table 3, Entry 15). Amines are singlet oxygen scavengers, and so the successful oxidation of methionine is remarkable result.

Furthermore, the recyclability of TPPS was tested over 5 cycles. To this aim, thioanisole (**39a**) was oxidized to the corresponding sulfidoxide (**40a**) (Table 3, Entry 1) and, upon completion, the corresponding sulfoxide was extracted with Me-THF, leaving the photosensitizer in the water phase. The organic phase were analyzed via ¹H qNMR technique to see the outcome of the reaction and the residual TPPS was concentrated and reused for the subsequent reaction.



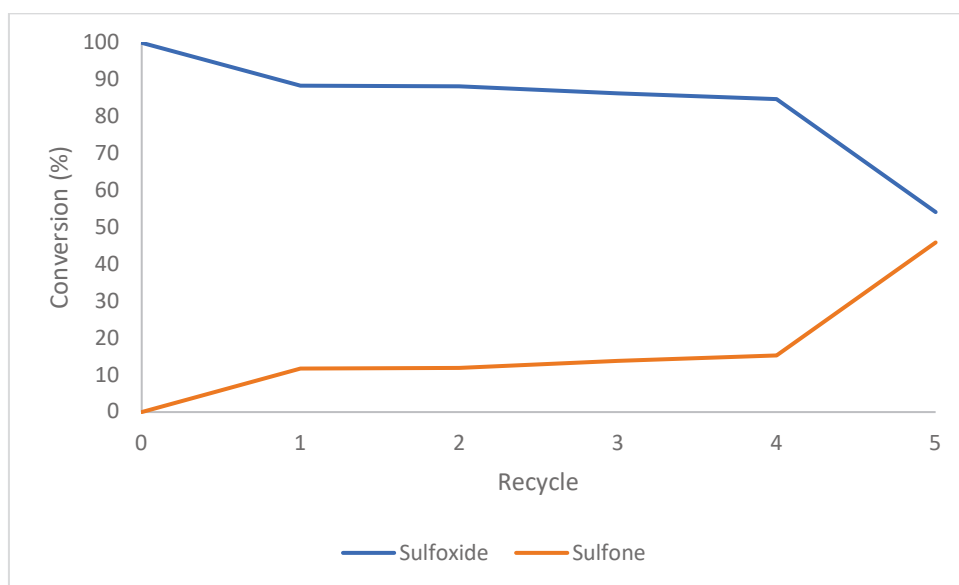


Figure 19: Selectivity loss study on recycled TPPS.

As depicted in Fig 19, there is a particular trend in the loss of selectivity when TPPS was recycled. The first oxidation resulted completely selective towards the sulfoxide (**40a**) with no sulfone (**43a**) detected. The second cycle showed a reduced selectivity, dropping down at a ratio of 85:15 in favour of the mono-oxidized compound. This ratio was confirmed during all next 3 recycling steps while the fifth recycle showed a further selectivity drops, reaching a ratio of 55:45 in favour of the sulfoxide, resulting in a non-selective photo-oxidation. Interestingly, the conversion remained almost complete after every cycle with no loss in activity of TPPS. At the moment this selectivity drops has not been fully understood, and further investigations are ongoing in our laboratories.

Methods

General procedure for the synthesis of sulfoxides (**40a-o**)

0.2 mmol of sulfide (**39a-o**) are loaded into a 4 mL vial and dissolved in the amount of ethanol determined via UV-vis spectroscopy (see below). When the solution is completely clear 1×10^{-4} mmol of TPPS are added from a mother solution prepared in sonicated water. Finally other sonicated water is added until 2 mL volume is reached. The vial prepared is insert in a metal support over a 3W LED (416 nm of maximum wavelength) at a distance of approximately 10

cm. A calibrated diode is used to determine the radiant flux before and after every reaction to keep the bottom of the vial irradiated with 10 mW. Compressed air is bubbled inside the vial using a syringe needle and a flowmeter is used to control the air flow. When the reaction is complete the solvent is removed and 15 mL of Me-THF are added, then the organic phases are extracted with water (3x15 mL) until the solution is colorless. The organic layers are then dried over sodium sulfate anhydrous and, upon filtration, the solvent is removed.

Preparation of the TPPS mother solution

1×10^{-2} mmol (10.2 mg) of 5,10,15,20-Tetraphenyl-21H, 23H-porphine-p,p',p,p''-tetrasulfonic acid tetrasodium hydrate (TPPS) are added to a 10 mL volumetric flask and accurately solubilized in water. Upon solubilization other water is added until the final volume of 10 mL is reached.

General procedure to recover the TPPS for recyclability studies

After the extraction with Me-THF, the residual aqueous phase are concentrated at rotavapor and added again to a freshly prepared sulfide solution and other water is added to reach 2 mL. After this the vial is positioned again in the metal support, ready for the following recycle step.

General procedure for the synthesis of sulfones (43a-o)

0.36 mmol of sulfide (**39a-o**) is added into a vial with a magnetic stirrer. The compound is solubilized in 5 mL of DCM and finally 1.11 mmol of 3-chlorobenzoperoxoic acid (MCPBA) are added to the solution and stirred for 8h at room temperature. After extraction with water (3*15 mL) the organic phases are dried over sodium sulfate anhydrous and the residual DCM is removed. To remove the last impurities a silica column chromatography can be used.

References

21. Ho, R. Y. N., Liebman, J. F. & Valentine, J. S. Active Oxygen in Chemistry. *Act. Oxyg. Chem.* 1–23 (1996) doi:10.1007/978-94-007-0874-7.
22. Handa, T. *et al.* Reactivity of singlet oxygen generated by the photosensitization of tetraphenylporphyrin in liposomes. *Colloid Polym. Sci.* **266**, 745–752 (1988).
23. Xin, J. *et al.* Comparison of the synergistic anticancer activity of ALPcS4 photodynamic therapy in combination with different low-dose chemotherapeutic agents on gastric cancer cells. *Oncol. Rep.* **40**, 165–178 (2018).
24. Lévesque, F. & Seeberger, P. H. Highly efficient continuous flow reactions using singlet oxygen as a ‘Green’ reagent. *Org. Lett.* **13**, 5008–5011 (2011).
25. Balzani, V., Ceroni, P., Juris, A.: Photochemistry and Photophysics concepts, research, applications, Weinheim, Germany: Wiley-VCH, 2014 [2015], pp. 176-178).
26. Greer, A. Christopher Foote’s discovery of the role of singlet oxygen [1O_2 ($^1\Delta_g$)] in photosensitized oxidation reactions. *Acc. Chem. Res.* **39**, 797–804 (2006).
27. E. J. Corey, Mukund M. Mehrotra, A. U. K. Generation of singlet O_2 from Triethylsilane and Ozone OK. *J. Chem. Inf. Model.* **53**, 1689–1699 (2013).
28. Ramos, S. M., Owrutsky, J. C. & Keehn, P. M. Increased stability of phosphite ozonides derived from 4-hydroxymethyl-1-phospha-2,6,7-trioxabicyclo[2.2.2]octane. *Tetrahedron Lett.* **26**, 5895–5898 (1985).
29. Mehta, G., Subramanian, U. R. & Pramanik, A. 1995 677. 677–678 (1995).
30. Prein, M. & Adam, W. The Schenck Ene Reaction: Diastereoselective Oxyfunctionalization with Singlet Oxygen in Synthetic Applications. *Angew. Chemie (International Ed. English)* **35**, 477–494 (1996).
31. Jiang, G., Chen, J., Huang, J. S. & Che, C. M. Highly efficient oxidation of amines to imines by singlet oxygen and its application in ugi-type reactions. *Org. Lett.* **11**, 4568–4571 (2009).

32. Gao, R. *et al.* Reaction of arylphosphines with singlet oxygen: Intra- vs intermolecular oxidation. *Org. Lett.* **3**, 3719–3722 (2001).
33. Jensen, F., Greer, A. & Clennan, E. L. Reaction of organic sulfides with singlet oxygen. A revised mechanism. *J. Am. Chem. Soc.* **120**, 4439–4449 (1998).
34. Salokhiddinov, K. I., Byteva, I. M. & Gurinovich, G. P. Lifetime of singlet oxygen in various solvents. *J. Appl. Spectrosc.* **34**, 561–564 (1981).
35. Khodaei, M. M., Bahrami, K. & Karimi, A. H₂O₂/Tf₂O system: An efficient oxidizing reagent for selective oxidation of sulfanes. *Synthesis (Stuttg)*. 1682–1684 (2008) doi:10.1055/s-2008-1067019.
36. Dambruoso, P. *et al.* TPPS supported on core-shell PMMA nanoparticles: The development of continuous-flow membrane-mediated electrocoagulation as a photocatalyst processing method in aqueous media. *Green Chem.* **17**, 1907–1917 (2015).

Photochemical reactions in aerosol condition

Even if the proposed method for the synthesis of sulfoxides in bulk condition is excellent both in terms of yield and time, superior performance may be obtained by working in aerosol condition. Aerosol photoreactors offer a promising alternative to the micro-structured or bulk photoreactors which can also distribute light effectively. In this reactor concept, droplets are generated by nebulizing a liquid reaction medium with a gas where each droplet act as a microreactor. When light hits a droplet, it is either absorbed or scattered and scattering depends on the relative sizes of the droplets and the wavelength of light as shown in Figure 20.

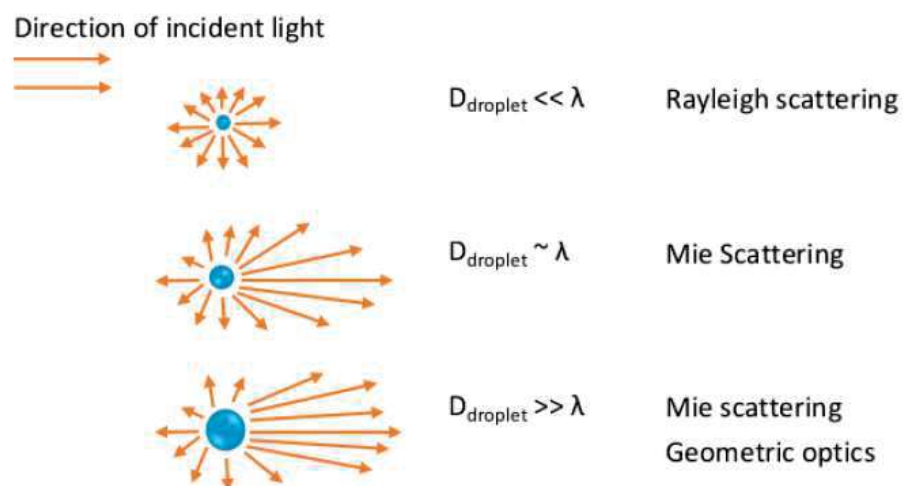
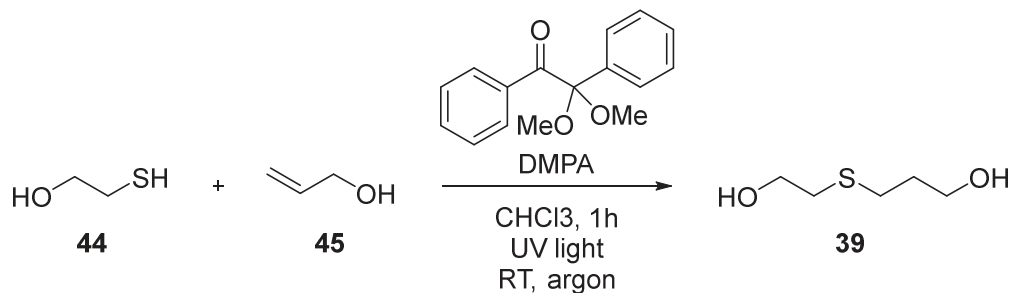


Figure 20: Droplet light interactions depend on the droplet diameter (D_{droplet}) and the wavelength of the incident light (λ).

For this purpose the research activities were divided into three different parts: firstly the kinetic studies of a model reaction in bulk phase to optimise the reaction conditions, then several trials in aerosol condition to obtain a proof of concept using easy-to-build reactors and finally the study of the model reaction in a lab-scale photoreactor.

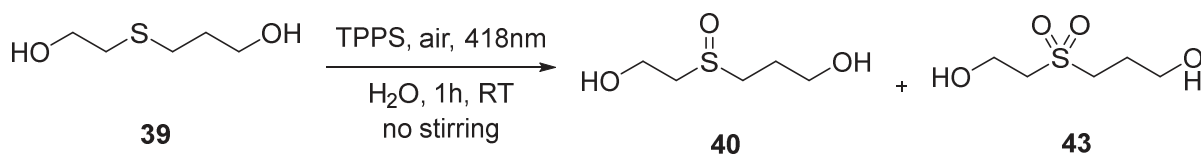
Due to the fact that aerosols are widely known to be explosive in presence of air, it was decided to work with an organic sulfide that is completely soluble in water to avoid any hazard. The selected molecule to perform the model reaction is the 3-((2-hydroxyethyl)thio)propan-1-ol (**39**) because it is widely known by the research group and respect the limits set. This sulfide is not

commercially available but it can be easily synthesized from 2-mercaptoethanol (**44**) and allylic alcohol (**45**) through a thiol-ene reaction catalysed by DMPA and UV light³⁷.



Reaction 12: *Synthesis of the model sulfide 39.*

The prepared sulfide **39** was then selectively photo-oxidated to the corresponding sulfoxide by singlet oxygen and TPPS as photosensitizer.



Reaction 13: *Bulk photo-oxidation of the model sulfide 39.*

The bulk optimization of the reaction is done by changing different parameters one by one and studying the reaction kinetics. To do so a 4 mL vial is placed on top of a LED at a fixed distance and pressurized air is flown inside the solution until complete conversion is reached (Reaction 13). At first air flow is kept at 100 mL/min and then increased at 160 mL/min, 220 mL/min and 300 mL/min.

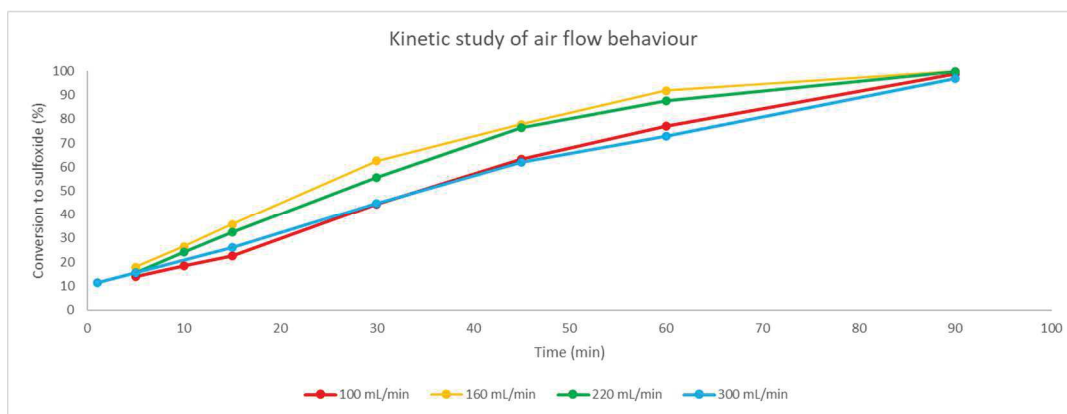


Figure 21: Kinetic study of air flow behaviour in bulk condition.

The kinetic study, reported in the graph above, shows how the air flow is not so impactful on the reaction outcome and so, with every air flow, almost complete conversion is reached after 90 minutes. That result can be interpreted as if singlet oxygen is generated in enough quantity at every air flow and it is not the limiting reagent. It was impossible to use air flow lower than 100 mL/min because the solvent surface tension prevents bubble formation.

At this point only TPPS concentration was left to be tested. All the previous reaction were carried on with the 0.02 mol% of catalyst compared to the sulfide quantity. By lowering or increasing the TPPS quantity it was impossible to find any substantial difference until 0.002 mol% was used and the reaction time increased slightly to 150 minutes to obtain full conversion. This information was important because it is directly connected to the Lambert-Beer equation:

$$A = \epsilon cL$$

TPPS, with its huge molar attenuation coefficient ($\epsilon=18900 \text{ cm}^{-1}/\text{M}$) absorbs light completely in just few mm of solution (L =optical path) and so concentration level of 10^{-3} M are enough to guarantee a satisfactory reaction outcome. Higher concentration of TPPS will reduce the optical path of the light while lower concentration worsen the reaction kinetics extending the time needed to reach complete conversion.

At this point the model reaction was performed in aerosol conditions using different homemade reactors with the aim of obtaining the first conversion data and an overall view of the difficulties and problems. Switching to a longer reactor was necessary to obtain valuable conversion and, even if the final mass recovery was insufficient, it was possible to selectively convert the 30%

of the sulfide to the sulfoxide with an average droplet lifetime of about 9 seconds. The acceleration factor in this case is calculated to be 200 compared to the bulk reaction. This outstanding result obviously needed to be confirmed in a more elegant way and so a cooperation with another research group was established.

This research group based in Leuven (Belgium) is composed by several chemical engineers with years of experience in reactor building and aerosol physics and is coordinated by associate professor Mumin Enis Leblebici. With their expertise it was possible to build an annular reactor with irradiation coming from the middle of it and big enough to allow an average droplet lifetime up to 24 seconds. From this collaboration a paper was published on Chemical Engineering Journal (impact factor of 13,273)³⁸. In this paper the approach to the model reaction was completely different from the one that has been explained in the last paragraphs. The focus of this study was closely linked to the fact that each microdroplet act as an independent reactor as shown in Figure 22.

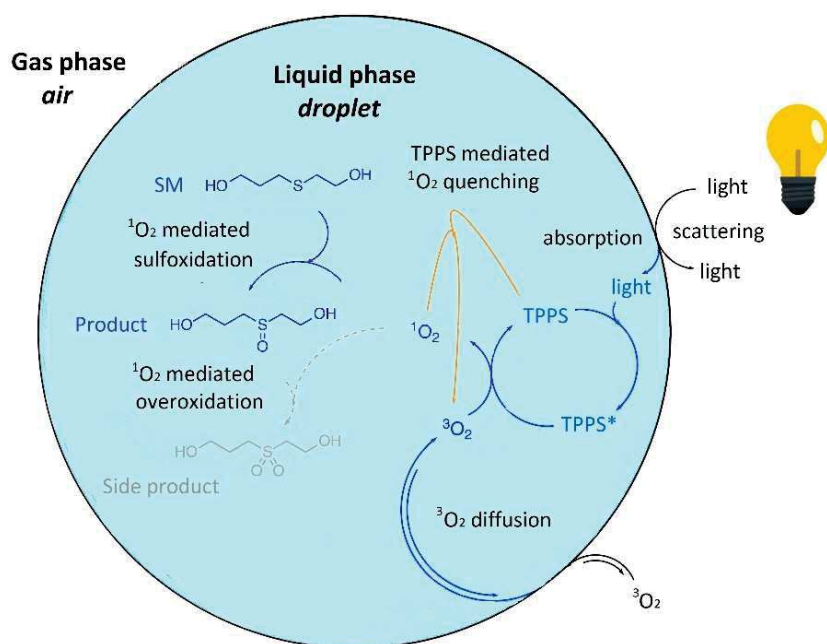


Figure 22: Representation of the physical and chemical phenomena involved in the photosulfoxidation reaction occurring inside a droplet.

Triplet oxygen ($^3\text{O}_2$) present in air diffuses in a liquid droplet. A violet light, with a 420 nm maximum emission peak, excites the photosensitizer (TPPS*) and then an energy transfer

process happens forming the singlet oxygen ($^1\text{O}_2$) and restoring the TPPS. The singlet oxygen is both responsible for the oxidation of the sulfide to the sulfoxide and to the sulfone. Overoxidation to sulfone is the side reaction of this process but was never observed during the experiments. TPPS concentration is key because singlet oxygen concentration increases with the TPPS concentration until a certain limit where generated $^1\text{O}_2$ is quenched back to inactive $^3\text{O}_2$ by excess TPPS.

From an experimental point of view all the reaction were carried out using the aerosol photoreactor shown in Figure 23.

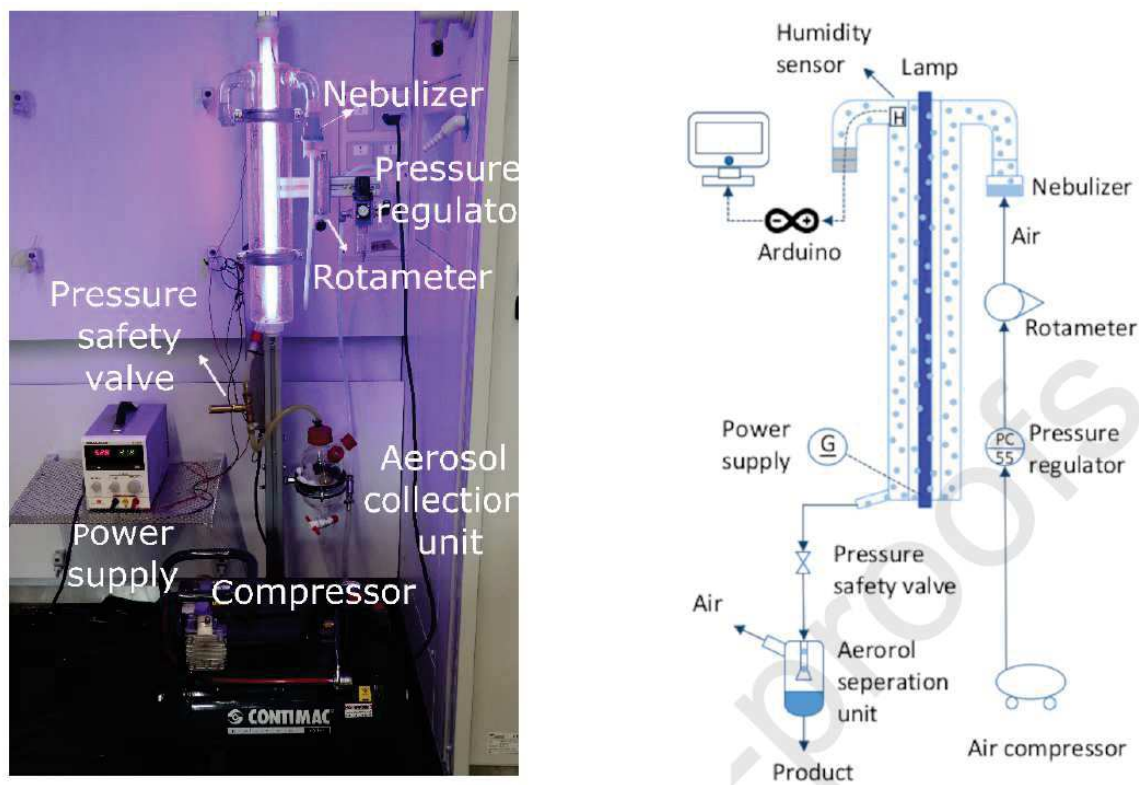
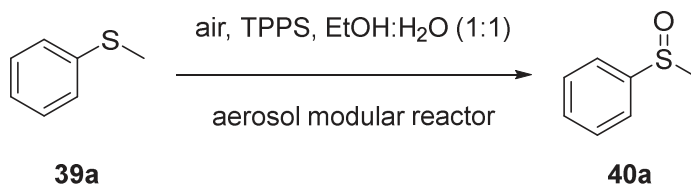


Figure 23: *Aerosol photoreactor on the left and the process flow chart of the setup on the right.*

An air compressor was used to supply air to a medical nebulizer and the pressure can be adjusted using a pressure regulator and a rotameter. For safety reason the aerosol reactor was equipped with a pressure safety valve. Product was collected without dilution from the aerosol collector unit that included a glass frit and a separating funnel. With a total volume of 1860 mL and a length of 50 cm the average microdroplet lifetime of 20 to 25 seconds was enough to obtain the selective oxidation of the sulfide with conversion around 95%.

The last part of this work was left unfinished. Aerosol photo-oxidation of organic sulfides in ethanol/water mixture has been studied partially. For instance, the modular reactor has been used to test the viability of the selective oxidation of thioanisole to the corresponding sulfoxide using TPPS as photosensitizer in a ethanol/water mixture (1:1).



Reaction 14: *Aerosol photooxidation of thioanisole 39a.*

The modular reactor was equipped with a medical glass nebulizer immersed in an oil bath to keep the temperature of the solution placed inside the nebulizer at 30°C. This was necessary because, when operating with a medical nebulizer, a severe cooling of the solution happens due to the reduced pressure generated by the air flow and the consequential solvent evaporation. The reduced temperature of the solution induces thioanisole precipitation and the formation of a heterogeneous solution. The modular reactor was also equipped with a lamp holder and four 3W LEDs with a maximum peak emission of 410 nm as shown in Figure 24.

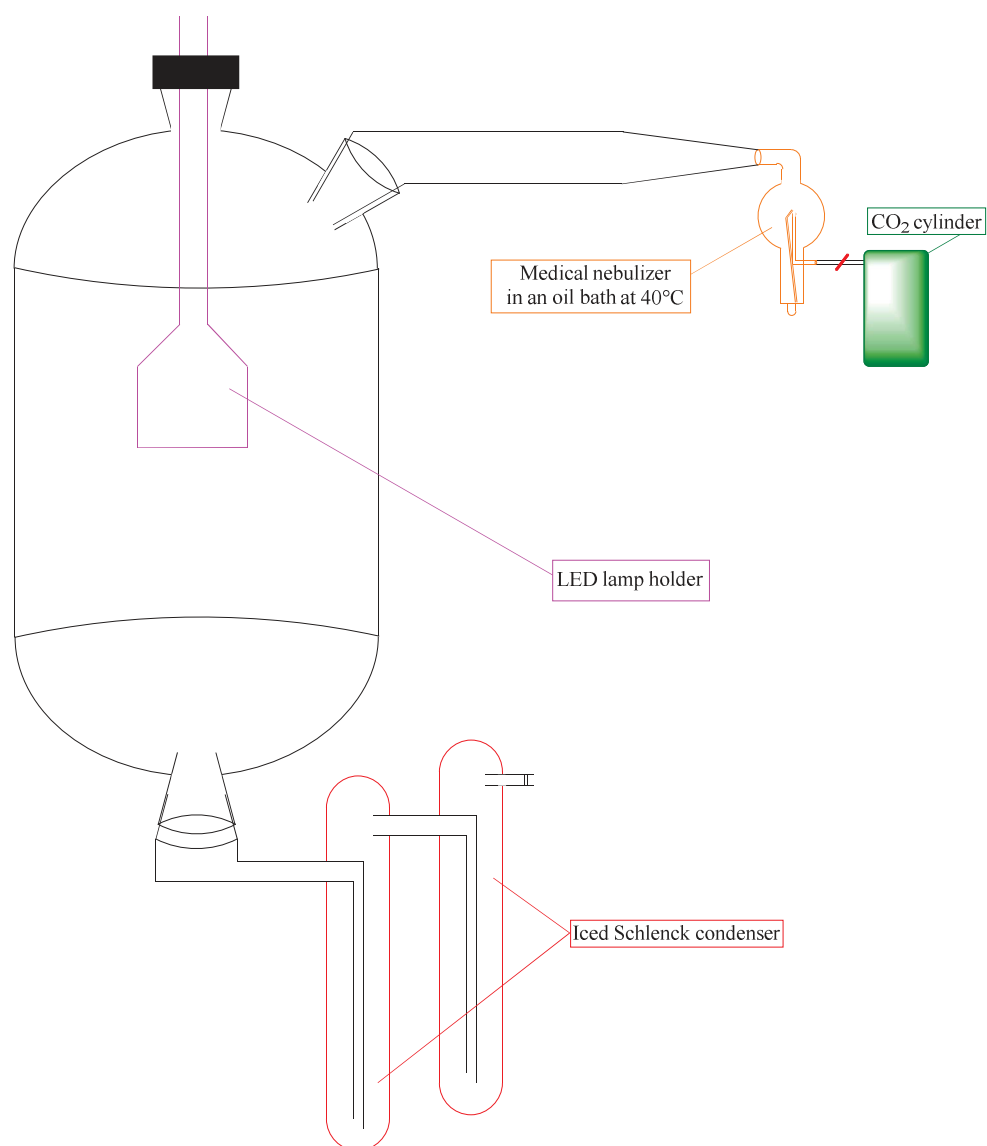


Figure 24: Modular aerosol reactor setup for photo-oxidation of organic sulfides.

The first trials were dedicated to the optimization of the setup conditions with a special focus on the final mass recovery of the product. The optimal approach was found out to be the nebulization of the solution from the top of the reactor with an air flow of approximately 750 mL/min at 1 bar and a double condenser unit made with two Schlenk tubes arranged in series. All this glassware was cooled in an icy water and salt solution (temperature around -15°C). The best result obtained for mass recovery was about 90% with complete conversion of the thioanisole. Due to an error in the design of the lamp holder no further experiment were carried out.

References

37. Hoyle, C. E. & Bowman, C. N. Thiol-ene click chemistry. *Angew. Chemie - Int. Ed.* **49**, 1540–1573 (2010).
38. Kayahan, E. *et al.* Overcoming mass and photon transfer limitations in a scalable reactor: Oxidation in an aerosol photoreactor. *Chem. Eng. J.* (2021) doi:10.1016/j.cej.2020.127357.

Carbon capture and utilization in bulk condition

Severe climate change represents a threat for human life, and its effects on environment, economic and social development is widely studied³⁹.

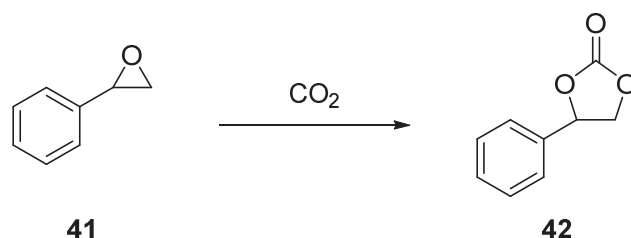
Unequivocally scientific evidences link climate change to greenhouse gases emissions, and identify CO₂ as a greenhouse gas. Two main technological approaches have been undertaken worldwide to tackle the CO₂ challenge and limit the increasing temperature to less than 2°C higher than pre-industrialization levels⁴⁰.

Carbon capture and storage (CCS) is the process of capturing carbon dioxide before it enters the atmosphere and, with different approaches, sequestering and storing it for centuries⁴¹. Carbon capture and utilization is, instead, the process of capturing the CO₂ with the aim of recycling it for further usage like fuel and chemical synthesis, carbon mineralization or algae cultivation⁴².

Various CO₂ utilization approaches have been identified and studied so far. Most of the reactions explored to date proceed in a gas-liquid biphasic mixture, where CO₂ in the gas phase should be initially absorbed into the liquid phase and, when dissolved therein, will react with the starting material to be transformed into the final product. A catalyst makes the transformation faster. Considering a catalyst very active in speeding up the reaction, the bottleneck of this process is the rate of CO₂ absorption in the liquid phase: a faster CO₂ absorption results in a quicker process. In the same way as a river fill a bottle with a larger neck faster than it does with the same bottle with a thinner one, CO₂ is absorbed faster in a certain volume of liquid when its surface exposed to the gas increases. On the other hand, like a pump empties the bottle faster than a pipette, a more active catalyst transforms faster the starting materials into the desired product. Particular attention should be paid to the pump selection: while a diesel pump pollutes the environment, an electric pump performs in the same way without affecting the surroundings. Accordingly, the catalyst selection should be carefully operated in order to repair, instead of shifting elsewhere, pollution issues. Finally, the amount of water retrieved from a bottle in certain time not only depends from the pump, but also from the filling/emptying procedure. A batchwise approach, in which the emptying phase follows the filling phase and does not start before the bottle is completely full allows to retrieve less water per unit time in respect of a continuous flow mode.

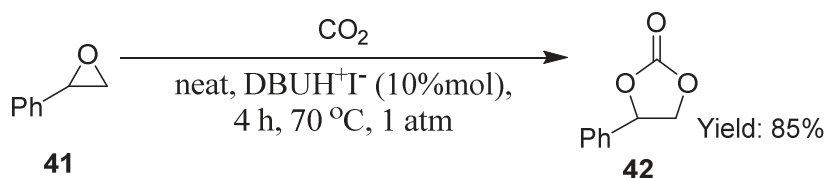
In three words, efficiency, productivity and sustainability issues are plaguing known CO₂ utilization approaches, and innovative ideas are needed to turn this polluting waste in a valuable feedstock.

As in the photooxidation exposed in previous chapters, also in this case it is important to approach the problem studying reaction behaviours in bulk conditions before focusing on the aerosol reaction. In this case no model reaction has been studied by the research group in previous occasion and so a wide study of the scientific literature was necessary to find a reaction with optimal characteristic. The chosen model reaction is the carbonatation of styrene oxide to obtain the styrene carbonate.



Reaction 15: Carbonatation reaction of styrene oxide (**41**) to obtain styrene carbonate (**42**).

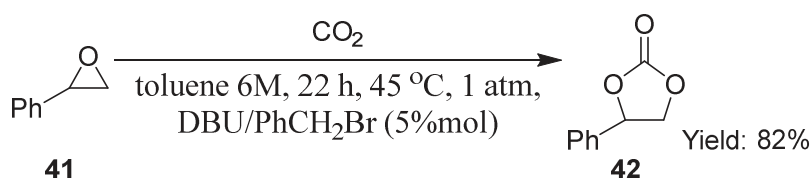
The aim of this preliminary study was the catalyst selection. Even if this reaction is widely reported, it usually requires high pressure and temperature to reach complete conversion in few hours. Obviously the kinetic study of a reaction that takes long time to reach complete conversion and has to be carried on with harsh conditions is not suitable for our aim. Moreover pressure and temperature are not parameter that can be easily changed with the current instrumental setup and involve expensive devices to be controlled in aerosol. Several catalyst were tried to see what is best for our setup. One of the constrains in choosing the catalyst is solubility in the reaction media. For example DBU salts (1,8-Diazabicyclo(5.4.0)undec-7-ene) are excellent catalyst for the synthesis of carbonates from CO₂ and epoxides⁴³.



Reaction 16: Cycloaddition of CO₂ to styrene oxide (**41**) catalysed by DBU iodide salt.

The synthesis of this type of catalyst can be done starting from DBU and ammonium halide in methanol with reflux condition overnight. The highest activity for the carboxylation of styrene oxide was done with the iodide salt of DBU ([HDBU]I) with final conversion up to 96% in just 4 hours. Reaction condition was 70°C and atmospheric pressure CO₂ without any solvent added. The catalyst loading between 1% and 10% were screened showing increase in the conversion with higher catalyst loading. This catalyst however was not suitable for our setup due to the insolubility of the DBU salt.

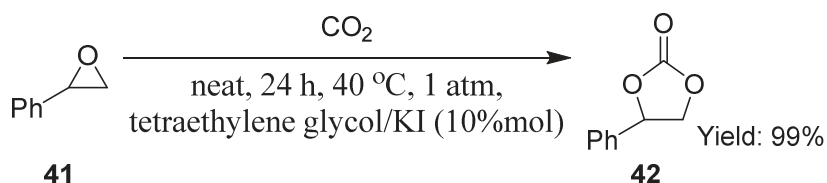
Another example is the synthesis of a wide range of cyclic carbonates using DBU and benzyl bromide as catalyst system⁴⁴.



Reaction 17: Cycloaddition of CO₂ to styrene oxide (**41**) catalysed by DBU Benzyl bromide.

In this case the catalyst was generated in situ and was completely soluble in styrene oxide without the need of any co-solvent addition. However this reaction, even if is possible at room temperature, is quite slow and reach a almost complete conversion only after 24 hours if ran at 65°C.

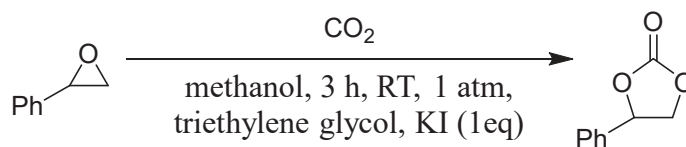
Last but not least a potassium iodide (KI) and triethylene glycol (TEG) catalyst was tested^{7,8}.



Reaction 18: Cycloaddition of CO₂ to styrene oxide (**41**) catalysed by KI/TEG complex.

In this case the complete solubility of the KI was ensured by TEG that can also be used in increased amount. Using the catalytic system at a 10% loading gave the possibility to obtain

styrene carbonate with a 27% yield in 24 hours at room temperature and atmospheric pressure CO₂. Increasing the concentration of both KI (1 equivalent compare to the styrene oxide) and TEG (to have complete solubility of the salt and an homogeneous solution) gave the possibility to obtain conversion in bulk condition up to 36% of the desired product. This reaction was selected as the model reaction for further studies.



Reaction 19: *Model reaction.*

The addition of methanol as a co-solvent was necessary due to the high viscosity of the bulk solution. Even if this is not a problem for the bulk phase reaction, the direct comparison with the aerosol version could be difficult and can lead to misinterpretation if the nebulization is not efficient. Several hypothesis for the reaction mechanism can be found in literature and are reported in Figure 25 and 26.

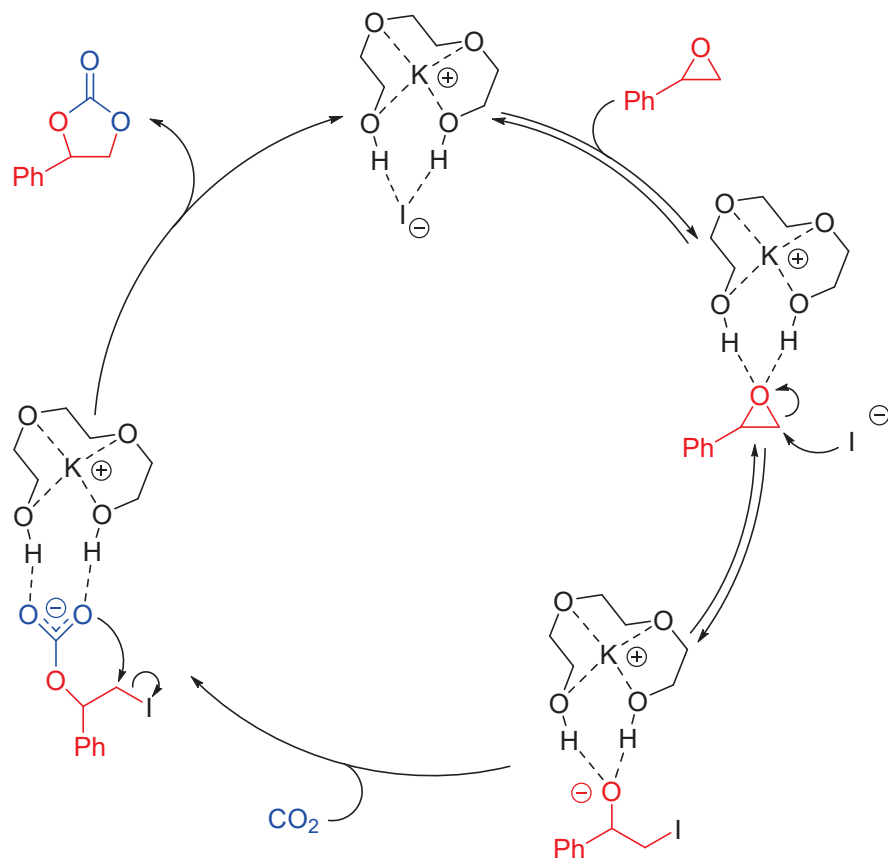


Figure 25: Kaneko's hypothesis of model reaction mechanism.

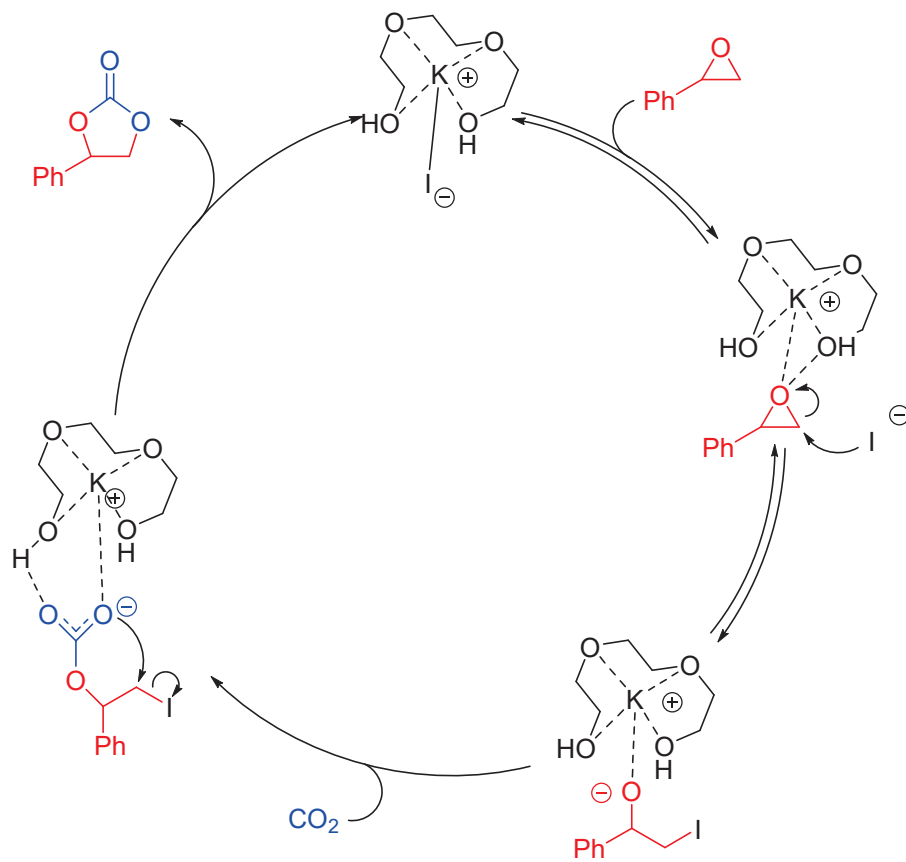


Figure 26: Butera's hypothesis of model reaction mechanism.

All the results obtained from the bulk condition approach will be reported in the next chapter as a direct comparison with the aerosol version of the model reaction.

References

39. Dong, K., Sun, R. & Dong, X. CO₂ emissions, natural gas and renewables, economic growth: Assessing the evidence from China. *Sci. Total Environ.* **640–641**, 293–302 (2018).
40. Haszeldine, S. R. Carbon Capture and Storage: How Green Can Black Be? *Science* (80- .). **325**, 1647–1652 (2009).
41. Bui, M. *et al.* Carbon capture and storage (CCS): The way forward. *Energy Environ. Sci.* **11**, 1062–1176 (2018).
42. Cuéllar-Franca, R. M. & Azapagic, A. Carbon capture, storage and utilisation technologies: A critical analysis and comparison of their life cycle environmental impacts. *J. CO₂ Util.* **9**, 82–102 (2015).
43. Fanjul-Mosteirín, N., Jehanno, C., Ruipérez, F., Sardon, H. & Dove, A. P. Rational Study of DBU Salts for the CO₂ Insertion into Epoxides for the Synthesis of Cyclic Carbonates. *ACS Sustain. Chem. Eng.* **7**, 10633–10640 (2019).
44. Wang, L., Kodama, K. & Hirose, T. DBU/benzyl bromide: An efficient catalytic system for the chemical fixation of CO₂ into cyclic carbonates under metal- and solvent-free conditions. *Catal. Sci. Technol.* **6**, 3872–3877 (2016).

Carbon capture and utilization in aerosol condition

The initial idea was to work with CO₂ in a flow reactor similar to the one used for the photo-oxidation of the organic sulfide. By the way several changes in the setup can be made. First of all the carbonatation of styrene oxide (**41**) does not require the presence of light and also required longer average droplet lifetime due to the lower reactivity of CO₂ compared to the singlet oxygen. For this reason an homemade reactor with two modified plastic bottle were attached from their bottom and used as a linear reactor (Figure 11). This approach was not satisfactory due to the high mass lost during the nebulization and an unsatisfactory conversion of the starting material in approximately 30 seconds of average microdroplet lifetime.

For this reason a batch aerosol setup was adopted for kinetic comparison between bulk and aerosol environment. The batch aerosol reactor was equipped with a ultrasonic water bath nebulizer and consist in a separating funnel place upside down. The close reactor can be filled with CO₂ and reacted solution can be recovered in a round bottom flask place on top of the reactor just by flipping the funnel to its normal position (Figure 12).

The kinetic comparison between bulk and aerosol conditions has been done evaluating the difference between several method of stirring the bulk solution versus the aerosol version at room temperature.

Table 4: Kinetic study of the model reaction in bulk condition without stirring.

BULK_RT_NO STIRRING					
Time (min)	Run 1	Run 2	Run 3	Average	Std.dev.
0	0,00	0,00	0,00	0,00	0,00
30	3,29	3,01	3,64	3,31	0,26
60	7,05	6,68	7,45	7,06	0,31
90	10,22	9,63	12,22	10,69	1,11
120	12,21	14,08	14,75	13,68	1,07
150	14,49	16,50	16,78	15,92	1,02
180	18,28	18,15	19,65	18,69	0,68

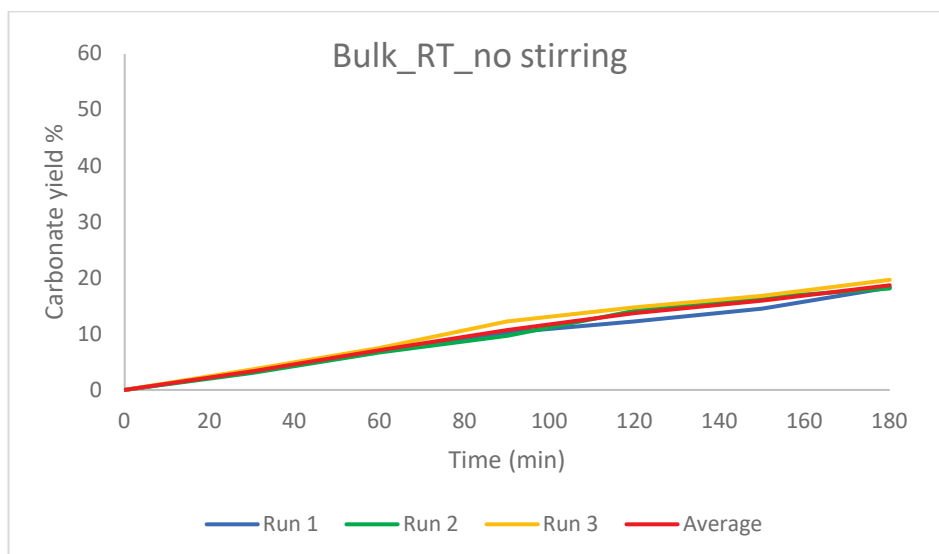


Table 5: Kinetic study of the model reaction in bulk condition with stirring.

BULK_RT_STIRRING					
Time (min)	Run 1	Run 2	Run 3	Average	Std.dev.
0	0,00	0,00	0,00	0,00	0,00
30	4,74	3,64	3,49	3,96	0,56
60	9,77	7,45	7,55	8,26	1,07
90	12,58	12,22	11,75	12,18	0,34
120	18,80	14,75	14,99	16,18	1,86
150	21,98	16,78	18,08	18,95	2,21
180	27,25	19,65	21,10	22,67	3,29

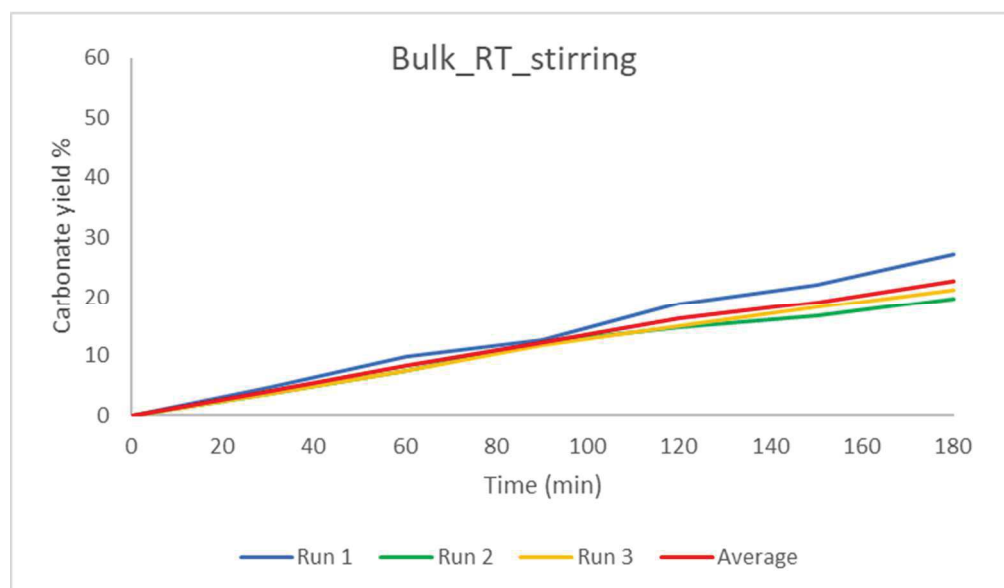
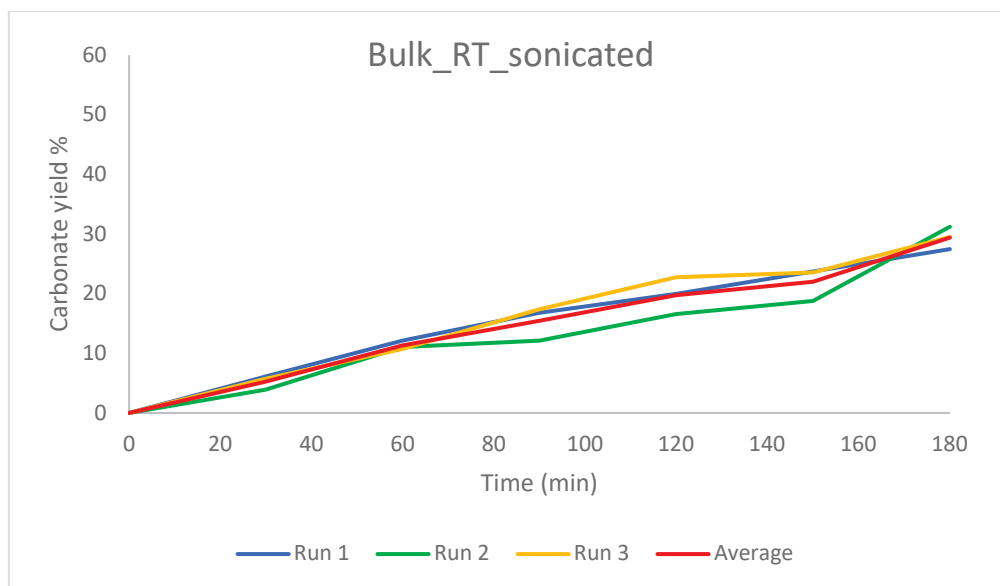


Table 6: Kinetic study of the model reaction in bulk condition with sonication.

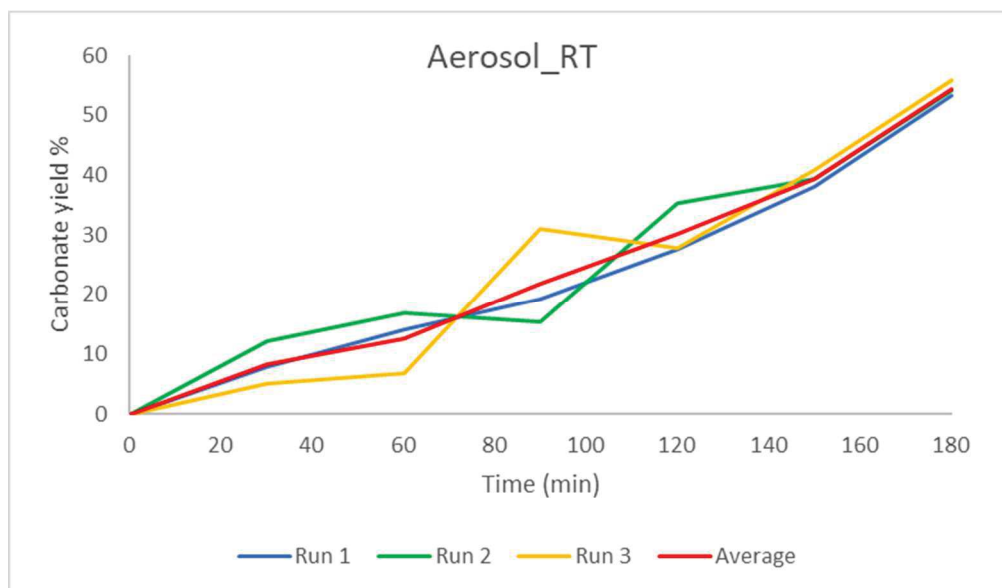
BULK_RT_SONICATION					
Time (min)	Run 1	Run 2	Run 3	Average	Std.dev.
0	0,00	0,00	0,00	0,00	0,00
30	6,10	3,92	5,75	5,26	0,96
60	12,09	11,05	10,73	11,29	0,58
90	16,78	12,11	17,36	15,42	2,35
120	19,92	16,58	22,73	19,74	2,51
150	23,70	18,76	23,53	22,00	2,29
180	27,47	31,25	29,50	29,41	1,54



This three different kinetic studies were necessary to take into account different ways of stirring the solution and to better understand the mass transfer limitations of the model reaction. When the solution was not stirred the average conversion obtained was 18,69% after 3 hours, while just by stirring the solution at 900 rpm the conversion increase to 22,67%. With regard to the sonication the same water bath used for aerosol nebulization was used, avoiding by any means the formation of microdroplets in the reaction flask. Furthermore ice and water were added every 5 minutes to the water bath to keep the room temperature steady.

Table 7: Kinetic study of the model reaction in aerosol condition.

AEROSOL_RT					
Time (min)	Run 1	Run 2	Run 3	Average	Std.dev.
0	0,00	0,00	0,00	0,00	0,00
30	7,84	12,14	5,15	8,38	2,88
60	14,08	16,92	6,67	12,56	4,32
90	19,23	15,43	30,96	21,87	6,61
120	27,47	35,21	27,70	30,13	3,60
150	38,17	39,37	40,82	39,45	1,08
180	53,19	54,05	55,87	54,37	1,12



Even if for the bulk reaction sampling every 30 minutes were done without any problems to analyse the solution and obtain conversion data, for the aerosol approach this was not possible and so every data corresponds to a different reaction. This can be easily seen in Table 7 through the variability of the data obtained. Also in this case the water bath was kept at room temperature in every reaction by the addition of ice and water. The average conversion obtained after 3 hours was of 54,37% with an increment of the 24,96% compared to the best bulk solution approach. The acceleration factor for the model reaction was of 1,85.

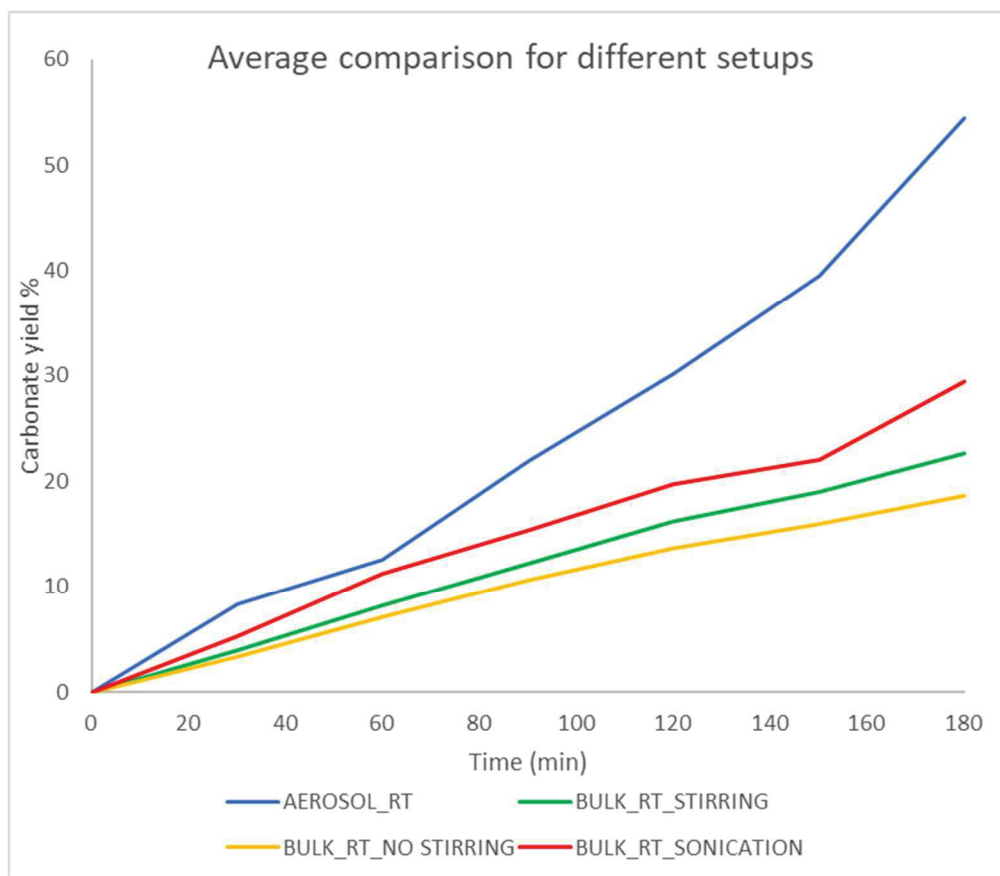
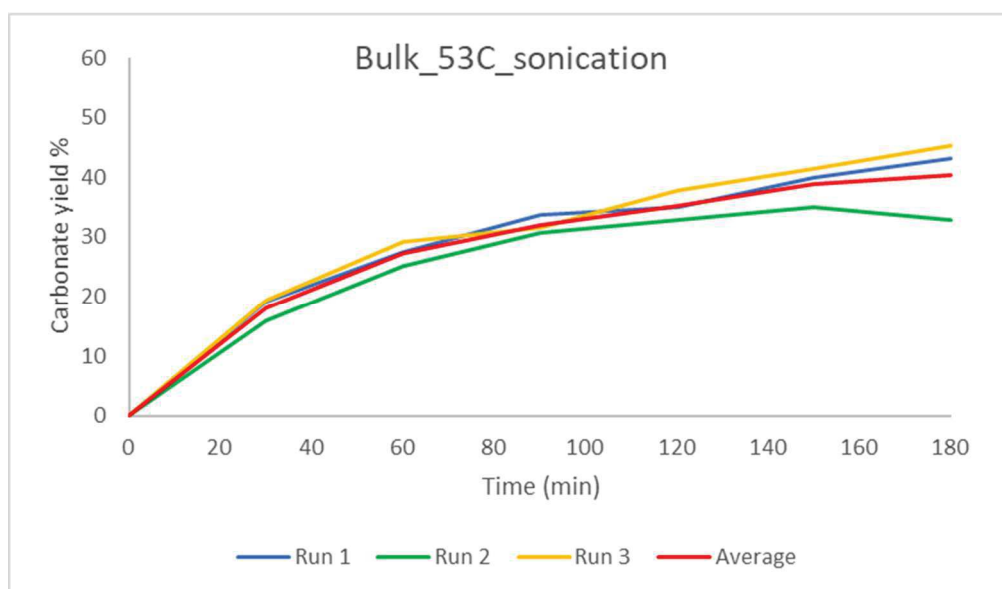


Figure 27: Comparison of the average run of each setup at room temperature.

The same kinetic study was repeated increasing the temperature to 53°C. An higher temperature can lead to better conversion as reported in literature^{45,46}.

Table 8: Kinetic study of the model reaction in bulk condition with sonication at 53°C.

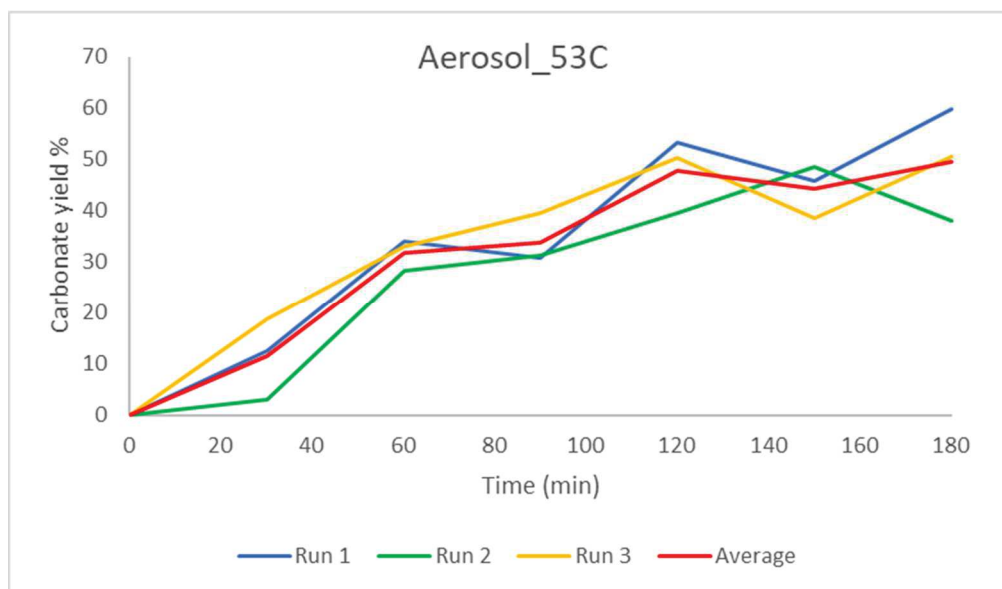
BULK_53C_SONICATION					
Time (min)	Run 1	Run 2	Run 3	Average	Std.dev.
0	0,00	0,00	0,00	0,00	0,00
30	19,16	15,85	19,27	18,09	1,59
60	27,47	25,06	29,32	27,28	1,74
90	33,67	30,67	31,64	31,99	1,25
120	35,09	32,79	37,74	35,21	2,02
150	40,00	34,96	41,49	38,82	2,79
180	43,10	32,79	45,25	40,38	5,44



As can be easily seen in the graph above the increased temperature increased the conversion in bulk condition when the solution is mixed by sonication. To the water bath hot water was added when necessary to keep the temperature steady. The average conversion was of 40,38% with an increase of 10,97% compared to the room temperature version of the model reaction.

Table 9: Kinetic study of the model reaction in aerosol condition at 53°C.

AEROSOL_53C					
Time (min)	Run 1	Run 2	Run 3	Average	Std.dev.
0	0,00	0,00	0,00	0,00	0,00
30	12,61	3,1	18,83	11,51	6,47
60	33,90	28,33	33,00	31,74	2,44
90	30,77	31,25	39,53	33,85	4,02
120	53,19	39,53	50,25	47,66	5,87
150	45,66	48,54	38,61	44,27	4,17
180	59,88	38,02	50,5	49,47	8,95



Heating an aerosol is quite difficult due to the high volume that has to be homogeneously heated. Nevertheless it was possible to achieve a good result by using two IR lamps placed one in front of the other with the reactor in the middle. Despite this the average conversion obtained was of 49,47% after 3 hours and it was worse that the room temperature version of the model reaction with a decrease of 4,90%.

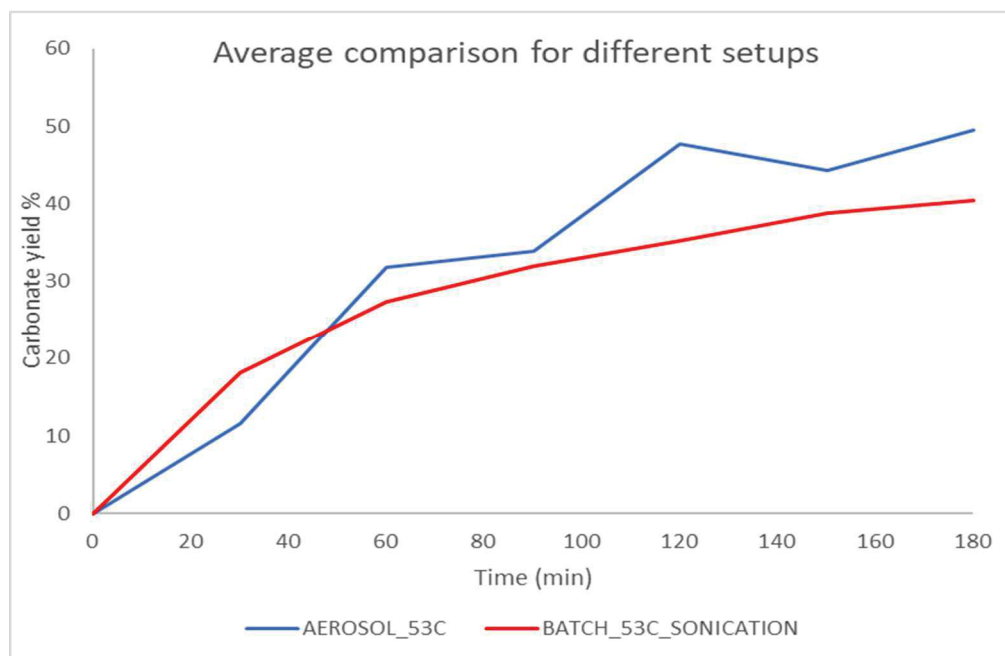


Figure 28: Comparison of the average run of each setup at 53°C.

Several studies were done to better understand why an higher temperature lead to different behaviours. Thinking about the two different environment were the model reaction takes place it was possible that a thermal degradation of the styrene carbonate can happen in each microdroplets due to solvent evaporation. To prove this, styrene carbonate was nebulized at 53°C in the same reaction media of the model reaction for 3 hours without the presence of the catalyst. From the analysis of the crude reaction no trace of the styrene oxide was found and so the higher temperature was not enough for carbonate direct degradation. And so, with the aim of fully understand this problem, styrene carbonate was this time nebulized at 53°C in the same reaction media of the model reaction for 3 hours with the presence of KI/TEG catalyst. In this case both the iodide intermediate (10,54%) and styrene oxide (60,32%) were found after analysis of the crude. Therefore, it has been established that no degradation of the carbonate occurs in microdroplets at 53°C but an inverse reaction catalysed by KI/TEG occurs and can explain the lower carbonate conversion at higher temperature. To complete this study both bulk and aerosol inverse reaction were carried on at room temperature and also at 53°C for the bulk reaction without finding any presence of styrene oxide or iodide intermediate.

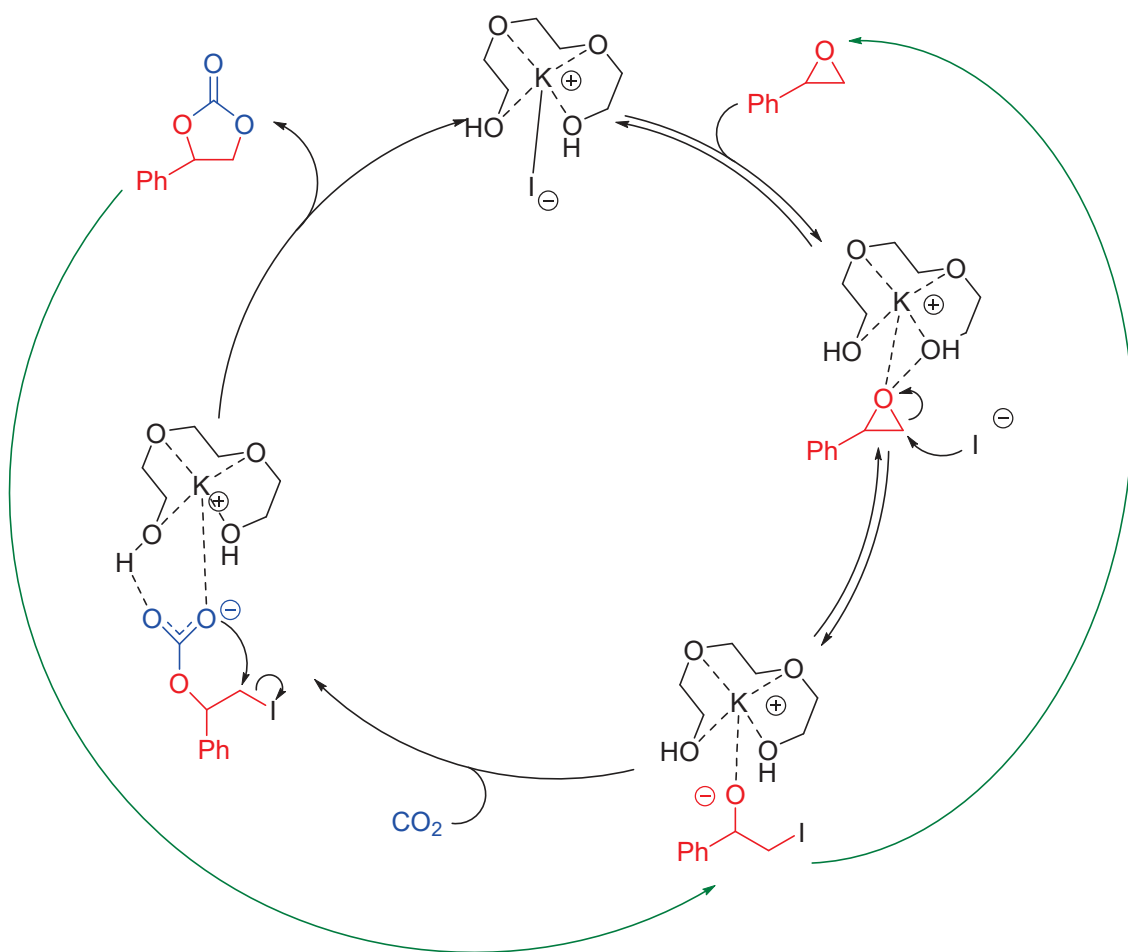


Figure 29: In green the possible inverse model reaction occurring at 53°C in aerosol condition based on Butera's hypothesis.

References

45. Kaneko, S. & Shirakawa, S. Potassium Iodide-Tetraethylene Glycol Complex as a Practical Catalyst for CO₂ Fixation Reactions with Epoxides under Mild Conditions. *ACS Sustain. Chem. Eng.* **5**, 2836–2840 (2017).
46. Butera, V. & Detz, H. Cyclic Carbonate Formation from Epoxides and CO₂ Catalyzed by Sustainable Alkali Halide-Glycol Complexes: A DFT Study to Elucidate Reaction Mechanism and Catalytic Activity. *ACS Omega* **5**, 18064–18072 (2020).

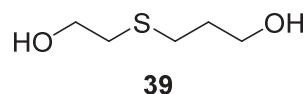
Conclusion

The photochemical oxidation of organic sulfides was extensively studied in bulk condition. The microdroplets study of the model reaction was fruitful and gave the possibility of better understand advantages and disadvantages of an aerosol flow reactor. The scope expansion of the photo-oxidation of organic sulfides not soluble in water is still challenging, but initial trials with the modular reactor designed and built at the end of the PhD period are encouraging.

CCU technologies are far more challenging than photochemical aerosol approach, however satisfactory results in terms of reaction acceleration and microdroplets behavior were obtained. Even if all the energies were focused on an aerosol batch reactor with all its limits, the modular reactor was designed mainly for the use of CO₂ as reactive carrier-gas in an aerosol flow reactor. Several data were collected with extreme difficulties, due to the novel approach choose on CCU technologies, and were sufficient to obtain a partnership for a NATO project call TANGO. The research group will now focus on the synthesis of new catalysts supported on magnetic nanoparticles that, hopefully, can convert styrene oxide into styrene carbonate with high yield and faster reaction time. All the experiments necessary are going to be exploiting the modular reactor designed and built with the experience gained on the strictly homogeneous reaction. The model reaction reported in this thesis will be the benchmark for future reactions.

Appendix

3-((2-hydroxyethyl)thio)propan-1-ol (**39**)

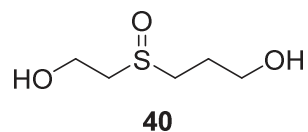


A mixture of 2-mercaptoethanol (**44**) (360 μ L, 5.12 mmol), prop-2-en-1-ol (**45**) (350 μ L, 5.12 mmol), 2,2-dimethoxy-2-phenyl-acetophenone (DMPA) (66 mg, 0.26 mmol), and chloroform (8.0 mL) was vigorously stirred, degassed under vacuum, and saturated with argon (by an Ar-filled balloon) three times. The mixture was irradiated (Philips CLEO 15W tube) at room temperature for 1 h under magnetic stirring, then 3.0 g of silica were added to the reaction mixture and the solvent was evaporated affording a white powder. This latter was charged on the top of a silica gel column and was purified by flash chromatography (stationary phase: 40 g of silica gel; eluting flow-rate: 40 mL/min; Collect wavelength 1: 254 nm; Collect wavelength 2: 280 nm). Elution gradient: from 30% to 100% of EtOAc in Cyclohexane for 5 CV; then neat EtOAc for 20 CV. Recovered 434 mg (2.9 mmol; yield: 62%) of 3-((2-hydroxyethyl)thio)propan-1-ol (**39**).

^1H NMR (500 MHz, CDCl_3): δ = 3.70 – 3.78 (m, 4 H), 2.73 (t, J = 6.0 Hz, 2 H), 2.66 (t, J = 7.1 Hz, 2 H), 2.34 (br. s, 2 H), 1.78 – 1.90 (m, 2 H) ppm.

^{13}C NMR (126 MHz, CDCl_3): δ = 61.6, 60.8, 35.4, 32.3, 28.6 ppm

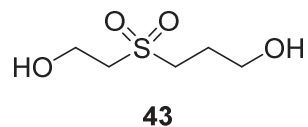
3-((2-hydroxyethyl)sulfinyl)propan-1-ol (**40**)



^1H NMR (500 MHz, D_2O): δ = 3.83 - 3.95 (m, 2 H), 3.62 (t, J = 6.5 Hz, 2 H), 2.97 - 3.07 (m, 1 H), 2.78 - 2.96 (m, 3 H), 1.83 - 1.93 (m, 2 H) ppm.

^{13}C NMR (126 MHz, D_2O): δ = 60.2, 54.9, 53.8, 48.0, 25.0 ppm.

3-((2-hydroxyethyl)sulfonyl)propan-1-ol (**43**)

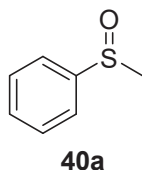


In a 25 mL round bottomed flask, 48.9 mg (0.36 mmol) of sulfide (**39**) were dissolved in 5 mL of CH₂Cl₂. Under vigorous magnetic stirring, 192 mg (1.11 mmol) of 3-chlorobenzoperoxoic acid (MCPBA) were added portion-wise to the reaction mixture. Vigorous gas evolution was observed. After 1.5 h, additional 192 mg (1.11 mmol) of MCPBA were added thereto. After 3 h, the reaction mixture was extracted with water (3 x 5 mL). The collected aqueous phases were free-dried to obtain 46 mg (0.27 mmol; yield 76%) of 3-((2-hydroxyethyl)sulfonyl)propan-1-ol (**43**).

¹H NMR (500 MHz, CDCl₃): δ = 4.13 – 4.19 (m, 2 H), 3.83 (t, J = 5.9 Hz, 2 H), 3.23 – 3.35 (m, 4 H), 2.08–2.20 (m, 2 H) ppm.

¹³C NMR (126 MHz, CDCl₃): δ = 60.8, 56.7, 55.5, 51.8, 25.0 ppm.

(Methylsulfinyl)benzene (40a)

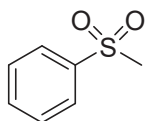


24 μL of thioanisole (**39a**) (0.2 mmol) were added to a 4 mL vial and solubilized in 1 mL of absolute ethanol. Then 0.9 ml of water and 100 μL of a mother solution of TPPS (10⁻³ mmol/mL) were added (final concentration of TPPS of 5*10⁻⁵ mmol/mL). The solution was continuously irradiated with a 3W high power LED (wavelength 416 nm, 10 mW radiant flux at the bottom of the vial) and compressed air was bubbled at 250 mL/min for 90 minutes. ¹H qNMR analysis of the crude gave a >99.5% conversion with no sulfone detected. The TPPS was separated from the product using Me-THF (3*15mL) and water and the organic layer was dried over Na₂SO₄ and concentrated. Column chromatography on SiO₂ with 100% EtOAc afforded 21 mg of sulfoxide (75% yield) as a pale yellow oil.

¹H NMR (500 MHz, CDCl₃) δ = 7.6 (m, 2H, Ar), 7.5 (m, 3H, Ar), 2.7 (s, 3H, CH₃) ppm.

¹³C NMR (126 MHz, CDCl₃) δ = 145.7, 131.0, 129.3, 123.5, 44.0 ppm.

(Methylsulfonyl)benzene (43a)



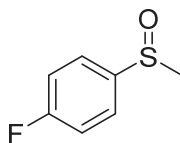
43a

44.7 μL of thioanisole (**39a**) (0.36 mmol) were added to a 10 mL vial and solubilized in 5 mL of DCM. Then 192 mg of MCPBA (1.11 mmol) were added to the solution and stirred vigorously overnight. The solution is then extracted with DCM and a 2% aqueous solution of NaOH (3x15 mL). The organic layer collected and dried over Na_2SO_4 . No further purification were needed, yield 55 mg (98%) as a white amorphous solid.

^1H NMR (300 MHz, CDCl_3) δ = 7.9 (m, 2H, Ar), 7.6 (m, 3H, Ar), 3.1 (s, 3H, CH_3) ppm.

^{13}C NMR (101 MHz, CDCl_3) δ = 140.5, 133.7, 129.3, 127.3, 44.5 ppm.

1-fluoro-4-(methylsulfinyl)benzene (**40b**)



40b

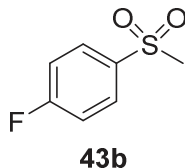
24 μL of (4-fluorophenyl)(methyl)sulfane (**39b**) (0.2 mmol) were added to a 4 mL vial and solubilized in 1 mL of absolute ethanol. Then 0.9 ml of water and 100 μL of a mother solution of TPPS (10^{-3} mmol/mL) were added (final concentration of TPPS of $5 \cdot 10^{-5}$ mmol/mL). The solution was continuously irradiated with a 3W high power LED (wavelength 416 nm, 10 mW radiant flux at the bottom of the vial) and compressed air was bubbled at 250 mL/min for 90 minutes. ^1H qNMR analysis of the solution gave a >99.5% conversion with no sulfone detected. The TPPS was separated from the product using Me-THF (3*15mL) and water and the organic layer was dried over Na_2SO_4 and concentrated. No further purification was needed and 28.5 mg of sulfoxide (90% yield) as a yellow solid was obtained.

^1H NMR (400 MHz, CD_3OD) δ = 7.7 (m, 2H, Ar), 7.2 (m, 2H, Ar), 2.7 (s, 3H, CH_3) ppm.

^{13}C NMR (126 MHz, CDCl_3) δ = 165.3, 163.3, 141.2, 141.1 125.9, 125.8, 116.8, 116.6, 44.2 ppm.

^{19}F NMR (470MHz, CDCl_3) $\delta = -108.6$ ppm.

1-fluoro-4-(methylsulfonyl)benzene (43b)



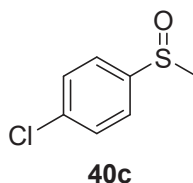
44 μL of (4-fluorophenyl)(methyl)sulfane (**39b**) (0.36 mmol) were added to a 10 mL vial and solubilized in 5 mL of DCM. Then 192 mg of MCPBA (1.11 mmol) were added to the solution and stirred vigorously overnight. The solution was then extracted with DCM and a 2% aqueous solution of NaOH (3x15 mL). The organic layer collected and dried over Na_2SO_4 . No further purification were needed, yield 59 mg (94%) as a white amorphous solid.

^1H NMR (300 MHz, CDCl_3) $\delta = 7.9$ (m, 2H, Ar), 7.2 (m, 2H, Ar), 3.0 (s, 3H, CH_3) ppm.

^{13}C NMR (101 MHz, CDCl_3) $\delta = 166.7, 164.7, 136.6, 136.6, 130.2, 130.2, 116.7, 116.5, 44.6$ ppm.

^{19}F NMR (376 MHz, CDCl_3) $\delta = -103.5$ ppm.

1-chloro-4-(methylsulfonyl)benzene (40c)



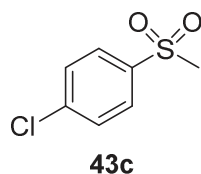
26 μL of (4-chlorophenyl)(methyl)sulfane (**39a**) (0.2 mmol) were added to a 4 mL vial and solubilized in 1.5 mL of absolute ethanol. Then 0.4 mL of water and 100 μL of a mother solution of TPPS (10^{-3} mmol/mL) were added (final concentration of TPPS of 5×10^{-5} mmol/mL). The solution was continuously irradiated with a 3W high power LED (wavelength 416 nm, 10 mW radiant flux at the bottom of the vial) and compressed air was bubbled at 250 mL/min for 180 minutes. ^1H qNMR analysis of the solution gave a >99.5% conversion with no sulfone detected.

The TPPS was separated from the product using Me-THF (3*15mL) and water and the organic layer was dried over Na₂SO₄ and concentrated. Column chromatography on SiO₂ with 100% EtOAc afforded 31.8 mg of sulfoxide (91% yield) as a colorless oil.

¹H NMR (400 MHz, CDCl₃) δ = 7.6 (m, 2H, Ar), 7.5 (m, 2H, Ar), 2.7 (s, 3H, CH₃) ppm.

¹³C NMR (126 MHz, CDCl₃) δ = 144.3, 137.2, 129.6, 124.9, 44.1 ppm.

1-chloro-4-(methylsulfonyl)benzene (43c)

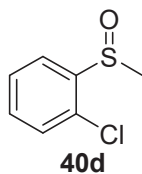


47 μL of (4-chlorophenyl)(methyl)sulfane (**39c**) (0.36 mmol) were added to a 10 mL vial and solubilized in 5 mL of DCM. Then 192 mg of MCPBA (1.11 mmol) were added to the solution and stirred vigorously overnight. The solution is then extracted with DCM and a 2% aqueous solution of NaOH (3x15 mL). The organic layer collected and dried over Na₂SO₄. No further purification were needed, yield 67 mg (98%) as a slightly yellow oil.

¹H NMR (300 MHz, CDCl₃) δ = 7.9 (m, 2H, Ar), 7.5 (m, 2H, Ar), 3.1 (s, 3H, CH₃) ppm.

¹³C NMR (126 MHz, CDCl₃) δ = 140.3, 138.9, 129.6, 128.8, 44.4 ppm.

1-chloro-2-(methylsulfinyl)benzene (40d)



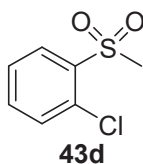
26 μL of (2-chlorophenyl)(methyl)sulfane (**39d**) (0.2 mmol) were added to a 4 mL vial and solubilized in 1.5 mL of absolute ethanol. Then 0.4 ml of water and 100 μL of a mother solution of TPPS (10⁻³ mmol/mL) were added (final concentration of TPPS of 5*10⁻⁵ mmol/mL). The solution was continuously irradiated with a 3W high power LED (wavelength 416 nm, 10 mW

radiant flux at the bottom of the vial) and compressed air was bubbled at 250 mL/min for 180 minutes. ^1H qNMR analysis of the solution gave a 63.9% conversion with no sulfone detected. The TPPS was separated from the product using Me-THF (3*15mL) and water and the organic layer was dried over Na_2SO_4 and concentrated. Column chromatography on SiO_2 with 30% EtOAc in cyclohexane afforded 19.2 mg of sulfoxide (55% yield) as a colorless oil.

^1H NMR (500 MHz, CDCl_3) δ = 8.0 (dd, 1H, Ar), 7.5 (dt, 1H, Ar), 7.4 (dt, 1H, Ar), 7.4 (dd, 1H, Ar), 2.8 (s, 3H, CH_3) ppm;

^{13}C NMR (126 MHz, CDCl_3) δ = 143.6, 131.9, 129.8, 129.7, 128.1, 125.3, 41.6 ppm.

1-chloro-2-(methylsulfonyl)benzene (43d)

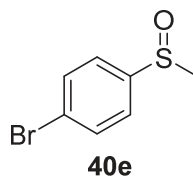


47 μL of (2-chlorophenyl)(methyl)sulfane (**39d**) (0.36 mmol) were added to a 10 mL vial and solubilized in 5 mL of DCM. Then 192 mg of MCPBA (1.11 mmol) were added to the solution and stirred vigorously overnight. The solution is then extracted with DCM and a 2% aqueous solution of NaOH (3x15 mL). The organic layer collected and dried over Na_2SO_4 . No further purification needed, yield 66 mg (96%) as a colorless oil.

^1H NMR (300 MHz, CDCl_3) δ = 8.2 (m, 1H, Ar), 7.6 (m, 2H, Ar), 7.5 (m, 1H, Ar), 3.3 (s, 3H, CH_3) ppm.

^{13}C NMR (126 MHz, CDCl_3) δ = 137.9, 134.7, 132.4, 131.8, 130.7, 127.4, 42.6 ppm.

1-bromo-4-(methylsulfinyl)benzene (40e)

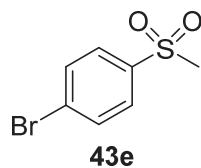


41 mg of (4-bromophenyl)(methyl)sulfane (**39e**) (0.2 mmol) were added to a 4 mL vial and solubilized in 1.8 mL of absolute ethanol. Then 0.1 ml of water and 100 μ L of a mother solution of TPPS (10^{-3} mmol/mL) were added (final concentration of TPPS of $5 \cdot 10^{-5}$ mmol/mL). The solution was continuously irradiated with a 3W high power LED (wavelength 416 nm, 10 mW radiant flux at the bottom of the vial) and compressed air was bubbled at 250 mL/min for 180 minutes. ^1H qNMR analysis of the solution gave a 90.1% conversion with no sulfone detected. The TPPS was separated from the product using Me-THF ($3 \cdot 15\text{mL}$) and water and the organic layer was dried over Na_2SO_4 and concentrated. Column chromatography on SiO_2 with 100% EtOAc afforded 34.1 mg of sulfoxide (78% yield) as a yellow amorphous solid.

^1H NMR (500 MHz, CDCl_3) δ = 7.7 (m, 2H, Ar), 7.5 (m, 2H, Ar), 2.7 (s, 3H, CH_3) ppm.

^{13}C NMR (126 MHz, CDCl_3) δ = 144.9, 132.6, 125.4, 125.1, 44.0 ppm.

1-bromo-4-(methylsulfonyl)benzene (**43e**)

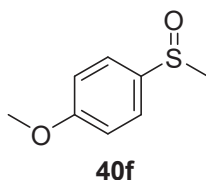


73 mg of (4-bromophenyl)(methyl)sulfane (**39e**) (0.36 mmol) were added to a 10 mL vial and solubilized in 5 mL of DCM. Then 192 mg of MCPBA (1.11 mmol) were added to the solution and stirred vigorously overnight. The solution is then extracted with DCM and a 2% aqueous solution of NaOH (3×15 mL). The organic layer collected and dried over Na_2SO_4 . No further purification were needed, yield 83 mg (98.5%) as a amorphous white solid.

^1H NMR (300 MHz, CDCl_3) δ = 7.8 (m, 2H, Ar), 7.7 (m, 2H, Ar), 3.1 (s, 3H, CH_3) ppm.

^{13}C NMR (126 MHz, CDCl_3) δ = 139.5, 132.7, 129.1, 129.0, 44.5 ppm.

1-methoxy-4-(methylsulfinyl)benzene (**40f**)

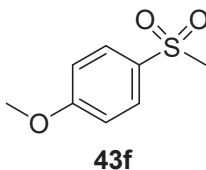


28 μL of (4-methoxyphenyl)(methyl)sulfane (**39f**) (0.2 mmol) were added to a 4 mL vial and solubilized in 1.5 mL of absolute ethanol. Then 0.4 mL of water and 100 μL of a mother solution of TPPS (10^{-3} mmol/mL) were added (final concentration of TPPS of $5 \cdot 10^{-5}$ mmol/mL). The solution was continuously irradiated with a 3W high power LED (wavelength 416 nm, 10 mW radiant flux at the bottom of the vial) and compressed air was bubbled at 250 mL/min for 180 minutes. ^1H qNMR analysis of the solution gave a 94.3% conversion with no sulfone detected. The TPPS was separated from the product using Me-THF ($3 \cdot 15\text{mL}$) and water and the organic layer was dried over Na_2SO_4 and concentrated. Column chromatography on SiO_2 with 100% EtOAc afforded 28.3 mg of sulfoxide (83% yield) as a white amorphous solid.

^1H NMR (500 MHz, CDCl_3) δ = 7.7 (m, 2H, Ar), 7.0 (m, 2H, Ar), 3.9 (s, 3H, CH_3); 2.7 (s, 3H, CH_3) ppm.

^{13}C NMR (126 MHz, CDCl_3) δ = 162.2, 136.7, 125.4, 114.8, 55.5, 44.0 ppm.

1-methoxy-4-(methylsulfonyl)benzene (43f)

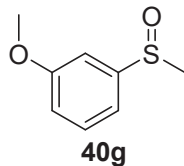


44.7 μL of (4-methoxyphenyl)(methyl)sulfane (**39f**) (0.36 mmol) were added to a 10 mL vial and solubilized in 5 mL of DCM. Then 192 mg of MCPBA (1.11 mmol) were added to the solution and stirred vigorously overnight. The solution is then extracted with DCM and a 2% aqueous solution of NaOH ($3 \cdot 15\text{mL}$). The organic layer collected and dried over Na_2SO_4 . No further purification were needed, yield 55 mg (98%) as a white amorphous solid.

^1H NMR (500 MHz, CDCl_3) δ = 7.9 (m, 2H, Ar), 7.0 (m, 2H, Ar), 3.9 (s, 3H, CH_3) 3.0 (s, 3H, CH_3) ppm.

^{13}C NMR (126 MHz, CDCl_3) δ = 163.7, 132.3, 129.5, 114.5, 55.7, 44.8 ppm.

1-methoxy-3-(methylsulfinyl)benzene (**40g**)

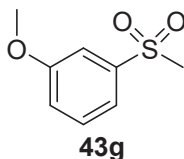


28 μL of (3-methoxyphenyl)(methyl)sulfane (**39g**) (0.2 mmol) were added to a 4 mL vial and solubilized in 1.5 mL of absolute ethanol. Then 0.4 mL of water and 100 μL of a mother solution of TPPS (10^{-3} mmol/mL) were added (final concentration of TPPS of $5 \cdot 10^{-5}$ mmol/mL). The solution was continuously irradiated with a 3W high power LED (wavelength 416 nm, 10 mW radiant flux at the bottom of the vial) and compressed air was bubbled at 250 mL/min for 90 minutes. ^1H qNMR analysis of the solution gave a 99.2% conversion with no sulfone detected. The TPPS was separated from the product using Me-THF ($3 \cdot 15\text{mL}$) and water and the organic layer was dried over Na_2SO_4 and concentrated. Column chromatography on SiO_2 with 70% EtOAc in cyclohexane afforded 29.3 mg of sulfoxide (86% yield) as a white amorphous solid.

^1H NMR (500 MHz, CDCl_3) δ = 7.4 (t, 1H, Ar), 7.3 (t, 1H, Ar), 7.1 (d, 1H, Ar), 7.0 (dd, 1H, Ar), 3.9 (s, 3H, CH_3), 2.7 (s, 3H, CH_3) ppm.

^{13}C NMR (126 MHz, CDCl_3) δ = 160.5, 147.1, 130.3, 117.5, 115.5, 107.9, 55.6, 44.0 ppm.

1-methoxy-3-(methylsulfonyl)benzene (**43g**)



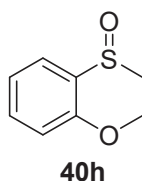
50 μL of (3-methoxyphenyl)(methyl)sulfane (**39g**) (0.36 mmol) were added to a 10 mL vial and solubilized in 5 mL of DCM. Then 192 mg of MCPBA (1.11 mmol) were added to the solution and stirred vigorously overnight. The solution is then extracted with DCM and a 2% aqueous

solution of NaOH (3x15 mL). The organic layer collected and dried over Na₂SO₄. No further purification were needed, yield 66 mg (98%) as a white amorphous solid.

¹H NMR (300 MHz, CDCl₃) δ = 7.5 (m, 3H, Ar), 7.2 (m, 1H, Ar), 3.9 (s, 3H, CH₃), 3.0 (s, 3H, CH₃) ppm.

¹³C NMR (101 MHz, CDCl₃) δ = 160.1, 141.7, 130.5, 120.1, 119.4, 111.8, 55.7, 44.4 ppm.

1-methoxy-2-(methylsulfinyl)benzene (40h)

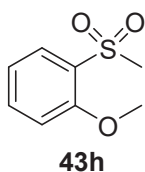


28 μL of (2-methoxyphenyl)(methyl)sulfane (**39h**) (0.2 mmol) were added to a 4 mL vial and solubilized in 1,5 mL of absolute ethanol. Then 0.4 ml of water and 100 μL of a mother solution of TPPS (10⁻³ mmol/mL) were added (final concentration of TPPS of 5*10⁻⁵ mmol/mL). The solution was continuously irradiated with a 3W high power LED (wavelength 416 nm, 10 mW radiant flux at the bottom of the vial) and compressed air was bubbled at 250 mL/min for 120 minutes. ¹H qNMR analysis of the solution gave a 99.4% conversion with no sulfone detected. The TPPS was separated from the product using Me-THF (3*15mL) and water and the organic layer was dried over Na₂SO₄ and concentrated. Column chromatography on SiO₂ with 70% EtOAc in cyclohexane afforded 27.6 mg of sulfoxide (81% yield) as a colorless oil.

¹H NMR (500 MHz, CDCl₃) δ = 7.8 (t, 1H, Ar), 7.5 (t, 1H, Ar), 7,2 (t, 1H, Ar), 6.9 (d, 1H, Ar), 3.9 (s, 3H, CH₃), 2.8 (s, 3H, CH₃) ppm.

¹³C NMR (126 MHz, CDCl₃) δ = 154.8, 132.0, 132.0, 124.7, 121.7, 110.6, 55.7, 41.1 ppm.

1-methoxy-2-(methylsulfonyl)benzene (43h)

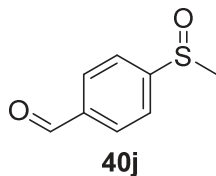


50 μ L of (2-methoxyphenyl)(methyl)sulfane (**39h**) (0.36 mmol) were added to a 10 mL vial and solubilized in 5 mL of DCM. Then 192 mg of MCPBA (1.11 mmol) were added to the solution and stirred vigorously overnight. The solution is then extracted with DCM and a 2% aqueous solution of NaOH (3x15 mL). The organic layer collected and dried over Na₂SO₄. No further purification were needed, yield 63.0 mg (95%) as a white amorphous solid.

¹H NMR (300 MHz, CDCl₃) δ = 8.0 (dd, 1H, Ar), 7.6 (m, 1H, Ar), 7.1 (m, 2H, Ar), 4.0 (s, 3H, CH₃), 3.2 (s, 3H, CH₃) ppm.

¹³C NMR (101 MHz, CDCl₃) δ = 157.2, 135.5, 129.7, 128.3, 120.7, 112.3, 56.3, 42.9 ppm.

4-(methylsulfinyl)benzaldehyde (40j)

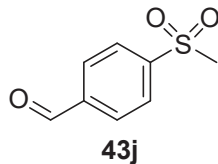


27 μ L of 4-(methylthio)benzaldehyde (**39j**) (0.2 mmol) were added to a 4 mL vial and solubilized in 1,5 mL of absolute ethanol. Then 0.4 ml of water and 100 μ L of a mother solution of TPPS (10⁻³ mmol/mL) were added (final concentration of TPPS of 5*10⁻⁵ mmol/mL). The solution was continuously irradiated with a 3W high power LED (wavelength 416 nm, 10 mW radiant flux at the bottom of the vial) and compressed air was bubbled at 250 mL/min for 120 minutes. ¹H qNMR analysis of the solution gave a 99.4% conversion with no sulfone detected. The TPPS was separated from the product using Me-THF (3*15mL) and water and the organic layer was dried over Na₂SO₄ and concentrated. Column chromatography on SiO₂ with 100% EtOAc afforded 35.0 mg of sulfoxide (95% yield) as a slightly yellow amorphous solid.

¹H NMR (500 MHz, CDCl₃) δ = 10.1 (s, 1H, HC=O), 8.1 (d, 2H, Ar), 7,8 (d, 2H, Ar), 2.8 (s, 3H, CH₃) ppm.

^{13}C NMR (126 MHz, CDCl_3) $\delta = 191.1, 152.5, 138.1, 130.4, 124.1, 43.8$ ppm.

4-(methylsulfonyl)benzaldehyde (43j)

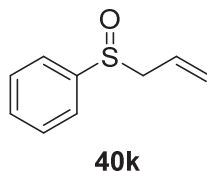


48 μL of (4-methylthio)benzaldehyde (**39j**) (0.36 mmol) were added to a 10 mL vial and solubilized in 5 mL of DCM. Then 192 mg of MCPBA (1.11 mmol) were added to the solution and stirred vigorously overnight. The solution is then extracted with DCM and a 2% aqueous solution of NaOH (3x15 mL). The organic layer collected and dried over Na_2SO_4 . No further purification were needed, yield 65.0 mg (98%) as a yellow amorphous solid.

^1H NMR (300 MHz, CDCl_3) $\delta = 10.1$ (s, 1H, $\text{HC}=\text{O}$), 8.1 (m, 4H, Ar), 3.1 (s, 3H, CH_3) ppm.

^{13}C NMR (101 MHz, CDCl_3) $\delta = 190.6, 145.3, 139.6, 130.4, 128.2, 44.3$ ppm.

(allylsulfinyl)benzene (40k)

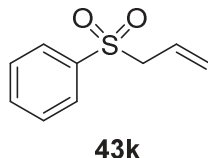


30 μL of Allyl(phenyl)sulfane (**39k**) (0.2 mmol) were added to a 4 mL vial and solubilized in 1,5 mL of absolute ethanol. Then 0.4 ml of water and 100 μL of a mother solution of TPPS (10^{-3} mmol/mL) were added (final concentration of TPPS of $5 \cdot 10^{-5}$ mmol/mL). The solution was continuously irradiated with a 3W high power LED (wavelength 416 nm, 10 mW radiant flux at the bottom of the vial) and compressed air was bubbled at 250 mL/min for 120 minutes. ^1H qNMR analysis of the solution gave a >99.5% conversion with a 3.4% of sulfone detected. The TPPS was separated from the product using Me-THF (3*15mL) and water and the organic layer was dried over Na_2SO_4 and concentrated. Column chromatography on SiO_2 with 20% EtOAc in cyclohexane afforded 29.2 mg of sulfoxide (88% yield) as a colorless oil.

^1H NMR (500 MHz, CD_3OD) δ = 7.7 (m, 2H, Ar), 7.6 (m, 3H, Ar), 5.7 (m, 1H, $\text{HC}=\text{C}$), 5.3 (m, 1H, $\text{H}_2\text{C}=\text{C}$), 5.2 (m, 1H, $\text{H}_2\text{C}=\text{C}$), 3.7 (dd, 1H, $\text{H}_2\text{CC}=\text{C}$), 3.6 (dd, 1H, $\text{H}_2\text{CC}=\text{C}$) ppm.

^{13}C NMR (126 MHz, CD_3OD) δ = 141.7, 131.2, 129.0, 125.1, 124.2, 123.1, 59.6 ppm.

(allylsulfonyl)benzene (**43k**)

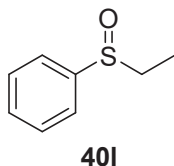


53 μL of Allyl(phenyl)sulfane (**39k**) (0.36 mmol) were added to a 10 mL vial and solubilized in 5 mL of DCM. Then 192 mg of MCPBA (1.11 mmol) were added to the solution and stirred vigorously overnight. The solution is then extracted with DCM and a 2% aqueous solution of NaOH (3x15 mL). The organic layer collected and dried over Na_2SO_4 . Column chromatography on SiO_2 with 10% EtOAc in cyclohexane afforded 61.0 mg (93% yield) as a colorless oil.

^1H NMR (500 MHz, CD_3OD) δ = 7.9 (m, 2H, Ar), 7.7 (m, 1H, Ar), 7.6 (m, 2H, Ar), 5.8 (m, 1H, $\text{HC}=\text{C}$), 5.3 (m, 1H, $\text{H}_2\text{C}=\text{C}$), 5.2 (m, 1H, $\text{H}_2\text{C}=\text{C}$), 4.0 (m, 2H, $\text{H}_2\text{C}-\text{S}$) ppm.

^{13}C NMR (126 MHz, CD_3OD) δ = 138.4, 133.6, 128.8, 128.1, 124.9, 123.5, 59.9 ppm.

(ethylsulfinyl)benzene (**40l**)



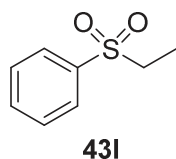
27 μL of Ethyl(phenyl)sulfane (**39l**) (0.2 mmol) were added to a 4 mL vial and solubilized in 1.5 mL of absolute ethanol. Then 0.4 mL of water and 100 μL of a mother solution of TPPS (10^3 mmol/mL) were added (final concentration of TPPS of $5 \cdot 10^{-5}$ mmol/mL). The solution was continuously irradiated with a 3W high power LED (wavelength 416 nm, 10 mW radiant flux at the bottom of the vial) and compressed air was bubbled at 250 mL/min for 120 minutes. ^1H

¹H NMR analysis of the solution gave a >99.5% conversion with a 7.4% of sulfone detected. The TPPS was separated from the product using Me-THF (3*15mL) and water and the organic layer was dried over Na₂SO₄ and concentrated. Column chromatography on SiO₂ with 50% EtOAc in cyclohexane afforded 21.6 mg of sulfoxide (70% yield) as a colorless oil.

¹H NMR (500 MHz, CDCl₃) δ = 7.7 (m, 2H, Ar), 7.6 (m, 3H, Ar), 3.0 (m, 1H, CH₂), 2.9 (m, 1H, CH₂), 1.2 (t, 3H, CH₃) ppm.

¹³C NMR (126 MHz, CDCl₃) δ = 142.0, 131.1, 129.1, 124.0, 49.4, 4.8 ppm.

(ethylsulfonyl)benzene (43l)

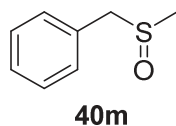


49 μL of Ethyl(phenyl)sulfane (**39l**) (0.36 mmol) were added to a 10 mL vial and solubilized in 5 mL of DCM. Then 192 mg of MCPBA (1.11 mmol) were added to the solution and stirred vigorously overnight. The solution is then extracted with DCM and a 2% aqueous solution of NaOH (3x15 mL). The organic layer collected and dried over Na₂SO₄. Column chromatography on SiO₂ with 20% EtOAc in cyclohexane afforded 58.2 mg (95% yield) as a colorless oil.

¹H NMR (500 MHz, CDCl₃) δ = 7.9 (m, 2H, Ar), 7.6 (m, 1H, Ar), 7.6 (m, 2H, Ar), 3.1 (q, 2H, CH₂), 1.3 (t, 3H, CH₃) ppm.

¹³C NMR (126 MHz, CDCl₃) δ = 138.5, 133.6, 129.2, 128.2, 50.6, 7.4 ppm.

((methylsulfinyl)methyl)benzene (40m)



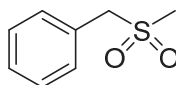
27 μL of Benzyl(methyl)sulfane (**39m**) (0.2 mmol) were added to a 4 mL vial and solubilized in 1,5 mL of absolute ethanol. Then 0.4 ml of water and 100 μL of a mother solution of TPPS

(10^{-3} mmol/mL) were added (final concentration of TPPS of $5 \cdot 10^{-5}$ mmol/mL). The solution was continuously irradiated with a 3W high power LED (wavelength 416 nm, 10 mW radiant flux at the bottom of the vial) and compressed air was bubbled at 250 mL/min for 90 minutes. ^1H qNMR analysis of the solution gave a >99.5% conversion with a 0.6% of sulfone detected. The TPPS was separated from the product using Me-THF (3*15mL) and water and the organic layer was dried over Na_2SO_4 and concentrated. Column chromatography on SiO_2 with 20% EtOAc in cyclohexane afforded 22.2 mg of sulfoxide (72% yield) as a white amorphous solid.

^1H NMR (500 MHz, CD_3OD) δ = 7.4 (m, 5H, Ar), 4.2 (q, 1H, CH_2), 4.1 (q, 1H, CH_2), 2.6 (s, 3H, CH_3) ppm.

^{13}C NMR (126 MHz, CD_3OD) δ = 130.1, 130.0, 128.4, 128.1, 58.6, 35.8 ppm.

((methylsulfonyl)methyl)benzene (43m)



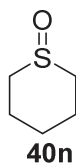
43m

49 μL of Benzyl(methyl)sulfane (**39m**) (0.36 mmol) were added to a 10 mL vial and solubilized in 5 mL of DCM. Then 192 mg of MCPBA (1.11 mmol) were added to the solution and stirred vigorously overnight. The solution is then extracted with DCM and a 2% aqueous solution of NaOH (3x15 mL). The organic layer collected and dried over Na_2SO_4 . Column chromatography on SiO_2 with 30% EtOAc in cyclohexane afforded 59.4 mg (97% yield) as a white amorphous solid.

^1H NMR (500 MHz, CD_3OD) δ = 7.5 (m, 5H, Ar), 4.5 (s, 2H, CH_2), 2.9 (s, 3H, CH_3) ppm.

^{13}C NMR (126 MHz, CD_3OD) δ = 131.2, 130.0, 129.0, 127.8, 38.6, 37.5 ppm.

Tetrahydro-2H-thiopyran 1-oxide (40n)

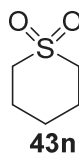


20.8 μL of Tetrahydro-2H-thiopyran (**39n**) (0.2 mmol) were added to a 4 mL vial and solubilized in 1 mL of absolute ethanol. Then 0.9 ml of water and 100 μL of a mother solution of TPPS (10^{-3} mmol/mL) were added (final concentration of TPPS of $5 \cdot 10^{-5}$ mmol/mL). The solution was continuously irradiated with a 3W high power LED (wavelength 416 nm, 10 mW radiant flux at the bottom of the vial) and compressed air was bubbled at 250 mL/min for 90 minutes. ^1H qNMR analysis of the solution gave a >99.5% conversion with no sulfone detected. The TPPS was separated from the product using Me-THF ($3 \cdot 15\text{mL}$) and water and the aqueous layer was liophilized overnight affording 18.4 mg of sulfoxide (78% yield) as a colorless oil.

^1H NMR (500 MHz, CD_3OD) δ = 3.0 (m, 2H), 2.8 (m, 2H), 2.2 (m, 2H), 1.7 (m, 4H) ppm.

^{13}C NMR (126 MHz, CD_3OD) δ = 72.4, 63.0, 23.8, 18.2 ppm.

Tetrahydro-2H-thiopyran 1,1-dioxide (**43n**)

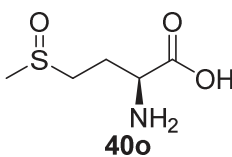


37 μL of Tetrahydro-2H-thiopyran (**39n**) (0.36 mmol) were added to a 10 mL vial and solubilized in 5 mL of DCM. Then 192 mg of MCPBA (1.11 mmol) were added to the solution and stirred vigorously overnight. The solution is then extracted with DCM and water ($1 \times 15\text{ mL}$). The aqueous layer was liophilized overnight affording 29.0 mg (60% yield) as a colorless oil.

^1H NMR (500 MHz, CDCl_3) δ = 3.0 (m, 4H), 2.1 (m, 4H), 1.6 (m, 2H) ppm.

^{13}C NMR (126 MHz, CDCl_3) δ = 48.8, 24.6, 19.1 ppm.

(2S)-2-amino-4-(methylsulfinyl)butanoic acid (**40o**)

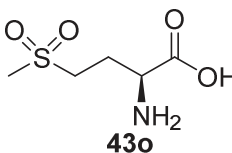


29.8 mg of L-methionine (**39n**) (0.2 mmol) were added to a 4 mL vial and solubilized in 1.9 mL of water. Then 100 μ L of a mother solution of TPPS (10^{-3} mmol/mL) were added (final concentration of TPPS of $5 \cdot 10^{-5}$ mmol/mL). The solution was continuously irradiated with a 3W high power LED (wavelength 416 nm, 10 mW radiant flux at the bottom of the vial) and compressed air was bubbled at 250 mL/min for 90 minutes. ^1H qNMR analysis of the solution gave a 97.1% conversion with no sulfone detected. The TPPS was separated from the product using Me-THF ($3 \cdot 15\text{mL}$) and water and the aqueous layer was lyophilized for 24h affording 21.4 mg of sulfoxide (65% yield) as a white amorphous solid.

^1H NMR (500 MHz, D_2O) δ = 3.8 (m, 1H), 2.9 (m, 2H), 2.6 (s, 3H, CH_3), 2.2 (m, 2H) ppm.

^{13}C NMR (126 MHz, D_2O) δ = 173.1, 53.3, 48.2, 36.5, 23.7 ppm.

(S)-2-amino-4-(methylsulfonyl)butanoic acid (**43o**)

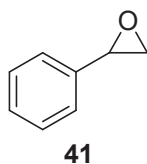


53.7 mg of L-methionine (**39o**) (0.36 mmol) were added to a 10 mL vial and solubilized in 5 mL of water. Then 192 mg of MCPBA (1.11 mmol) were added to the solution and stirred vigorously overnight. The solution is then extracted with DCM and water (1×15 mL). The aqueous layer was lyophilized overnight affording 48.9 mg (75% yield) as a white amorphous solid.

^1H NMR (500 MHz, D_2O) δ = 3.8 (t, 1H, CH-N), 3.3 (m, 2H, CH_2), 3.0 (s, 3H, CH_3), 2.3 (m, 2H, CH_2) ppm.

^{13}C NMR (126 MHz, D_2O) δ = 172.8, 53.5, 49.8, 40.2, 23.1 ppm.

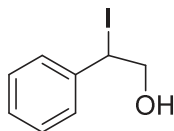
2-phenyloxirane (**41**)



^1H NMR (500 MHz, CDCl_3) δ = 7.39-7.30 (m, 5H, Ar), 3.88 (dd, 1H, CH, $J_{\text{CH-CH}_2}$ =3.96, $J_{\text{CH-CH}_2'}$ =2.67), 3.16 (dd, 1H, CH_2 , $J_{\text{CH}_2\text{-CH}_2'}$ =5.46, $J_{\text{CH}_2\text{-CH}}$ =4.16), 2.82 (dd, 1H, CH_2' , $J_{\text{CH}_2'\text{-CH}_2}$ =5.50, $J_{\text{CH}_2'\text{-CH}}$ =2.58) ppm.

^{13}C NMR (500 MHz, CDCl_3) δ = 137.55 (Ar ipso), 128.42 (Ar *meta*), 128.10 (Ar *para*), 125.42 (Ar *ortho*), 52.27 (CH), 51.11 (CH_2) ppm.

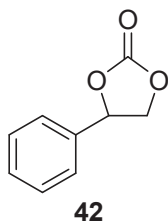
2-iodo-2-phenylethan-1-ol



^1H NMR (500 MHz, CDCl_3) δ = 7.37-7.30 (m, 5H, Ar), δ 4.81 (dd, 1H, CH, $J_{\text{CH-CH}_2'}$ =8.23, $J_{\text{CH-CH}_2}$ =3.50), 4.76 (broad s, 1H, OH), 3.75 (dd, 1H, CH_2' , $J_{\text{CH}_2\text{-CH}_2'}$ =11.42, $J_{\text{CH}_2\text{-CH}}$ =3.50), 3.65 (dd, 1H, CH_2' , $J_{\text{CH}_2'\text{-CH}_2}$ =11.35, $J_{\text{CH}_2'\text{-CH}}$ =8.27) ppm.

^{13}C NMR (500 MHz, CDCl_3) δ = 140.43 (Ar ipso), 128.51 (Ar *meta*), 127.97 (Ar *para*), 126.03 (Ar *ortho*), 74.54 (CH), 67.90 (CH_2) ppm.

4-phenyl-1,3-dioxolan-2-one (**42**)



^1H NMR (500 MHz, CDCl_3) δ = 7.46-7.36 (m, 5H, Ar), δ 5.68 (t, 1H, CH, $J_{\text{CH-CH}_2}$ = $J_{\text{CH-CH}_2'}$ =8.01), 4.81 (t, 1H, CH_2 , $J_{\text{CH}_2\text{-CH}_2'}$ = $J_{\text{CH}_2\text{-CH}}$ =8.40), 4.35 (t, 1H, CH_2' , $J_{\text{CH}_2'\text{-CH}_2}$ =

$\text{CH}_2=\text{JCH}_2'-\text{CH}=8.29$) ppm.

^{13}C NMR (500 MHz, CDCl_3) δ = 154.77 (OCOO), 135.76 (Ar ipso), 129.68 (Ar *meta*), 129.18 (Ar *para*), 125.82 (Ar *ortho*), 77.94 (CH), 71.11 (CH_2) ppm.



Università
degli Studi
di Ferrara

Sezioni

Dottorati di ricerca

Il tuo indirizzo e-mail

rbndnl@unife.it

Oggetto:

Dichiarazione di conformità della tesi di Dottorato

Io sottoscritto Dott. (Cognome e Nome)

Urbani Daniele

Nato a:

San Remo

Provincia:

Imperia

Il giorno:

10/06/1992

Avendo frequentato il Dottorato di Ricerca in:

Scienze Chimiche

Ciclo di Dottorato

34

Titolo della tesi:

Overcoming light and mass transfer phenomena in gas-liquid biphasic reactions: introduction of the aerosol methodological paradigm

Titolo della tesi (traduzione):

Superamento dei fenomeni di trasferimento di luce e massa nelle reazioni bifasiche gas-liquido: introduzione al paradigma metodologico dell'aerosol

Tutore: Prof. (Cognome e Nome)

Bortolini Olga

Settore Scientifico Disciplinare (S.S.D.)

CHIM/06

Parole chiave della tesi (max 10):

Aerosol, singlet oxygen, carbon dioxide, green chemistry, flow reactor

Consapevole, dichiara

CONSAPEVOLE: (1) del fatto che in caso di dichiarazioni mendaci, oltre alle sanzioni previste dal codice penale e dalle Leggi speciali per l'ipotesi di falsità in atti ed uso di atti falsi, decade fin dall'inizio e senza necessità di alcuna formalità dai benefici conseguenti al provvedimento emanato sulla base di tali dichiarazioni; (2) dell'obbligo per l'Università di provvedere al deposito di legge delle tesi di dottorato al fine di assicurarne la conservazione e la consultabilità da parte di terzi; (3) della procedura adottata dall'Università di Ferrara ove si richiede che la tesi sia consegnata dal dottorando in 2 copie di cui una in formato cartaceo e una in formato pdf non modificabile su idonei supporti (CD-ROM, DVD) secondo le istruzioni pubblicate sul sito: <http://www.unife.it/studenti/dottorato> alla voce ESAME FINALE – disposizioni e modulistica; (4) del fatto che l'Università, sulla base dei dati forniti, archiverà e renderà consultabile in rete il testo completo della tesi di dottorato di cui alla presente dichiarazione attraverso l'Archivio istituzionale ad accesso aperto "EPRINTS.unife.it" oltre che attraverso i Cataloghi delle Biblioteche Nazionali Centrali di Roma e Firenze; DICHIARO SOTTO LA MIA RESPONSABILITA': (1) che la copia

della tesi depositata presso l'Università di Ferrara in formato cartaceo è del tutto identica a quella presentata in formato elettronico (CD-ROM, DVD), a quelle da inviare ai Commissari di esame finale e alla copia che produrrò in seduta d'esame finale. Di conseguenza va esclusa qualsiasi responsabilità dell'Ateneo stesso per quanto riguarda eventuali errori, imprecisioni o omissioni nei contenuti della tesi; (2) di prendere atto che la tesi in formato cartaceo è l'unica alla quale farà riferimento l'Università per rilasciare, a mia richiesta, la dichiarazione di conformità di eventuali copie; (3) che il contenuto e l'organizzazione della tesi è opera originale da me realizzata e non compromette in alcun modo i diritti di terzi, ivi compresi quelli relativi alla sicurezza dei dati personali; che pertanto l'Università è in ogni caso esente da responsabilità di qualsivoglia natura civile, amministrativa o penale e sarà da me tenuta indenne da qualsiasi richiesta o rivendicazione da parte di terzi; (4) che la tesi di dottorato non è il risultato di attività rientranti nella normativa sulla proprietà industriale, non è stata prodotta nell'ambito di progetti finanziati da soggetti pubblici o privati con vincoli alla divulgazione dei risultati, non è oggetto di eventuali registrazioni di tipo brevettale o di tutela. PER ACCETTAZIONE DI QUANTO SOPRA RIPORTATO

Firma del dottorando

Ferrara, li 28/02/2022 (data) Firma del Dottorando

Damiano Urbani

Firma del Tutore

Visto: Il Tutore Si approva Firma del Tutore _____

O. Bello